Imidazo[1,2-a]quinoxalines for melanoma treatment with original mechanism of action

Cindy Patinote, Carine Deleuze-Masquéfa, Kamel Hadj Kaddour, Laure-Anaïs Vincent, Romain Larive, Zahraa Zghaib, Jean-François Guichou, Mona Diab Assaf, Pierre-Antoine Bonnet

Version of Record: https://www.sciencedirect.com/science/article/pii/S0223523420310035
Manuscript_0677fbdcb6f30bb54e24d65b92e58d79

Imidazo[1,2-*a*]quinoxalines for melanoma treatment with original mechanism of action.

Cindy Patinote[1,2,a], Carine Deleuze-Masquéfa[1,a,*], Kamel Hadj Kaddour[1], Laure-Anaïs Vincent[1], Romain Larive[1], Zahraa Zghaib[1,3], Jean-François Guichou[4], Mona Diab Assaf[3], Pierre Cuq[1], Pierre-Antoine Bonnet[1].

1. Institut des Biomolécules Max Mousseron (IBMM), UMR 5247, CNRS, Université de Montpellier, Faculté de Pharmacie, 15 avenue Charles Flahault, BP 14491, 34093 Montpellier Cedex 5, France.
2. Société d'Accélération du Transfert de Technologies (SATT AxLR), CSU, 950 rue Saint Priest, 34090 Montpellier, France.
3. Tumorigenèse et Pharmacologie Antitumorale, Lebanese University, EDST, BP 90656, Fanar Jdeideh, Lebanon.
4. CNRS, UMR 5048, INSERM, U105, Université de Montpellier, Centre de Biochimie Structurale, 34090 Montpellier, France

a. These authors contribute equally to this work.

* Corresponding author: carine.masquefa@umontpellier.fr

Abstract

The malignant transformation of melanocytes causes several thousand deaths each year, making melanoma an important public health concern. Melanoma is the most aggressive skin cancer, which incidence has regularly increased over the past decades. We described here the preparation of new compounds based on the 1-(3,4-dihydroxyphenyl)imidazo[1,2-*a*]quinoxaline structure. Different positions of the quinoxaline moiety were screened to introduce novel substituents in order to study their influence on the biological activity. Several alkylamino or alkyloxy groups were also considered to replace the methylamine of our first generation of Imiqualines. Imidazo[1,2-*a*]pyrazine derivatives were also designed as potential minimal structure. The investigation on A375 melanoma cells displayed interesting *in vitro* low nanomolar cytotoxic activity. Among them, **9d** (**EAPB02303**) is particularly remarkable since it is 20 times more potent than vemurafenib, the reference clinical therapy used on BRAF mutant melanoma. Contrary to the first generation, **EAPB02303** does not inhibit tubulin polymerization, as confirmed by an *in vitro* assay and a molecular modelisation study. The mechanism of action for **EAPB02303** highlighted by a transcriptomic analysis is clearly different from a panel of 12 well-known anticancer drugs. *In vivo* **EAPB02303** treatment reduced tumor size and weight of the A375 human melanoma xenografts in a dose-dependent manner, correlated with a low mitotic index but not with necrosis.

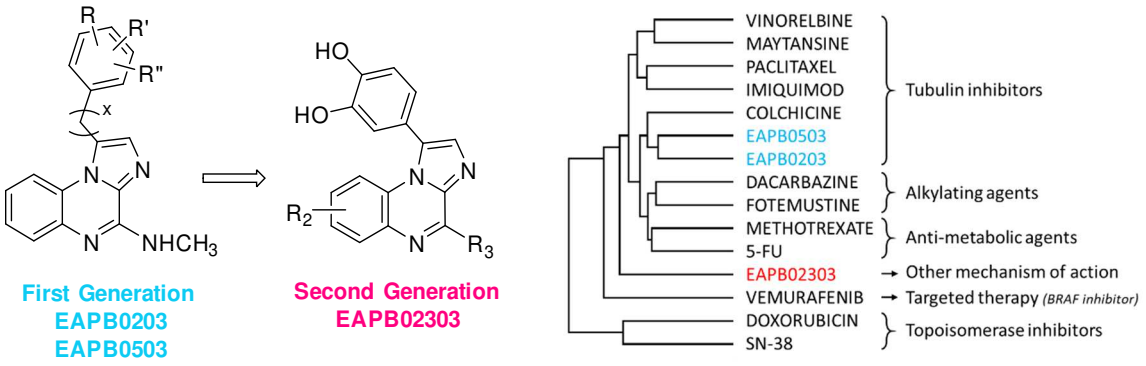

Keywords

Imidazo[1,2-*a*]quinoxaline, Imidazo[1,2-*a*]pyrazine, Imiqualines, Melanoma, A375 cells.

1. Introduction

Melanoma, the sixth most frequently diagnosed cancer and the most dangerous and aggressive skin cancer, corresponds to the degeneration of pigment-containing cells (melanocytes) into cancer cells. This malignant cancer spreads quite early to others organs by metastases during the vertical growth phase. The management of melanoma depends greatly on the location, depth and stage.[8] While early stages can achieve remarkable outcomes with surgery alone, metastatic melanoma requires therapeutic treatment intervention, such as chemotherapeutic agents, targeted therapies (Vemurafenib for BRAF mutation[13], dabrafenib[14], trametinib[15] and cobimetinib[16] for MEK inhibitors[17]) or immunotherapies (prembrolizumab, nivolumab as PD-1 inhibitors[21], ipilimumab as CTLA-4 inhibitors[22], cytokines (IFN-α, IL-2)[23]). Although a steady improvement in survival among patients has been reported over the last decades thanks to essentially early detection, therapy improvement and diagnosis, the mortality rates from melanoma continue to rise in several European countries due to an increasing incidence.[5,6] There is always a need for the discovery of new therapeutic compounds.[7]

Originally developed as nucleoside analogue with antiviral properties, Imiquimod is a member of the immune response modifier family (Scheme 1). [26] The interesting activity of this drug prompted us to synthetize novel analogues in the pyrazoloquinoxaline and imidazoquinoxaline families. The first generation of Imiqualines was essentially substituted on position 1 by multiple aromatic moieties directly grafted to the main structure or via an alkyl linker.[27–30] Our Imiqualines first generation were characterized by significant anti-cancer activities with ICs_{50} in the μM range against a large variety of cancer cell lines and the most active derivatives were found to interact with tubulin. Such interaction is detrimental for further development since tubulin is present in all cancer as well as normal cells. For further development of the series, it was important to study the possibility to disconnect the anticancer activity from the tubulin interaction, which is a non-specific inhibition. In order to explore this potential anti-cancer activity of our compounds, we first undertook a molecular modelling study with the aim of finding a substituted phenyl to get rid off the interaction in the colchicin site of the tubulin. These results allowed us to synthesize and develop a second generation of Imiqualines which is characterized by the presence of the 3,4-dihydroxyphenyl moiety on position 1. We present herein the design of new compounds belonging to the imidazo[1,2-*a*]quinoxaline and imidazo[1,2-*a*]pyrazine series and their *in vitro* results. The mechanism of action of the best compound to date EAPB02303 (9d) has been envisaged, as well as preliminary *in vivo* evaluation to treat melanoma.

2. Results and discussion

We previously synthesized a panel of imidazo[1,2-*a*]quinoxaline derivatives exhibiting remarkable anti-proliferative effects on human melanoma cell line A375 (Scheme 1). Among this first series of potent anti-cancer compounds, the most active compound **EAPB0503** showed also potent inhibition of tubulin polymerization.[31,32] Molecular docking simulations revealed that EAPB0503 was able to make a hydrogen bond with ASP682A and Van der Waals contacts with VAL174A, ASN689B, ALA747B, ILE749B, LYS783B and ALA785B in the colchicine binding site of tubulin (Figure 1). The quantitative analyses of the interaction estimate a binding free energy of -8.5 kcal/mol with a contribution of -1.2 kcal/mol of the hydrogen bond, this result demonstrates a high contribution of

the Van der Waals contacts for the interaction of EAPB0503 with tubulin. The binding to tubulin was experimentally determined in *vitro* (see 2.2.). Even if tubulin targeting agents have played a key role in cancer treatment, colchicine binding site inhibitors have not yet reached the commercial phase.[33] That is why focusing on the anti-cancer property while being free from any tubulin targeting property could be the new insight into the design of new agents.

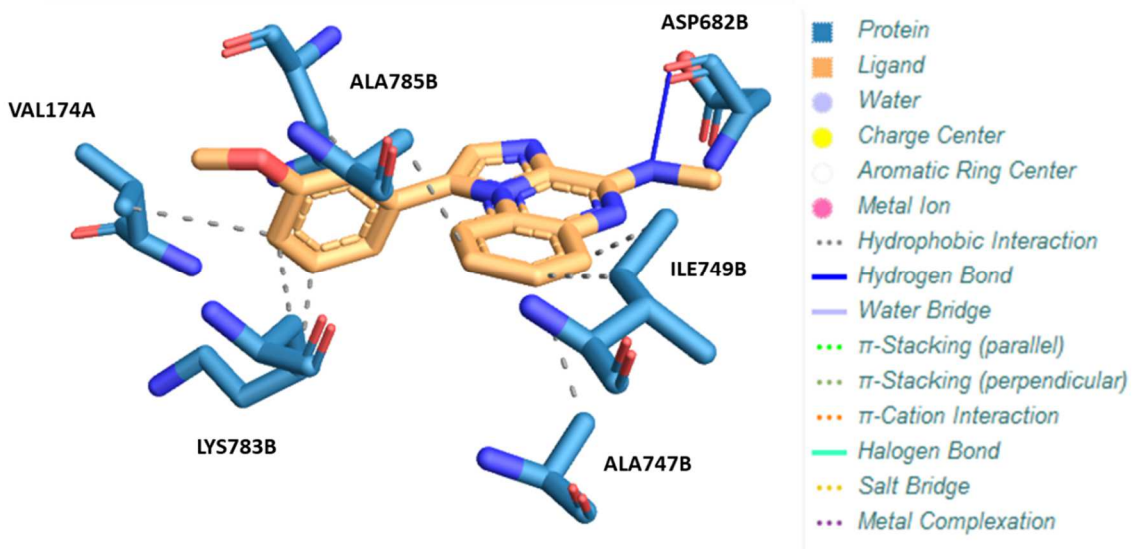

Figure 1: Analyses of the EAPB0503 interaction with the colchicine site.

2.1. Molecular docking: design of the novel Imiqualines generation.

In order to further explore the potential variability of Imiqualines to interact with the colchicine site of tubulin, we underwent several molecular docking simulations based on the structure of our hit **EAPB0503** using analogues with a variety of substituents. These simulations exhibited high binding discrepancies between imidazoquinoxalines bearing methoxy or hydroxyl groups on the aromatic moiety fixed on position 1 of the tricyclic heterocycle. Actually, the presence of a catechol group on position 1 was found to be highly detrimental for the virtual docking within the colchicine site. With this dihydroxyphenyl moiety, we determined no binding in the tubulin colchicine site compared to the results obtained with the first generation Imiqualines with one methoxy group such as our hit **EAPB0503** (Figure 2). This result can be explained since the driving forces of the EAPB0503 interaction with tubulin are Van der Waals contacts. The introduction of two hydroxyl groups induces polarity which is highly unfavorable to such interaction.

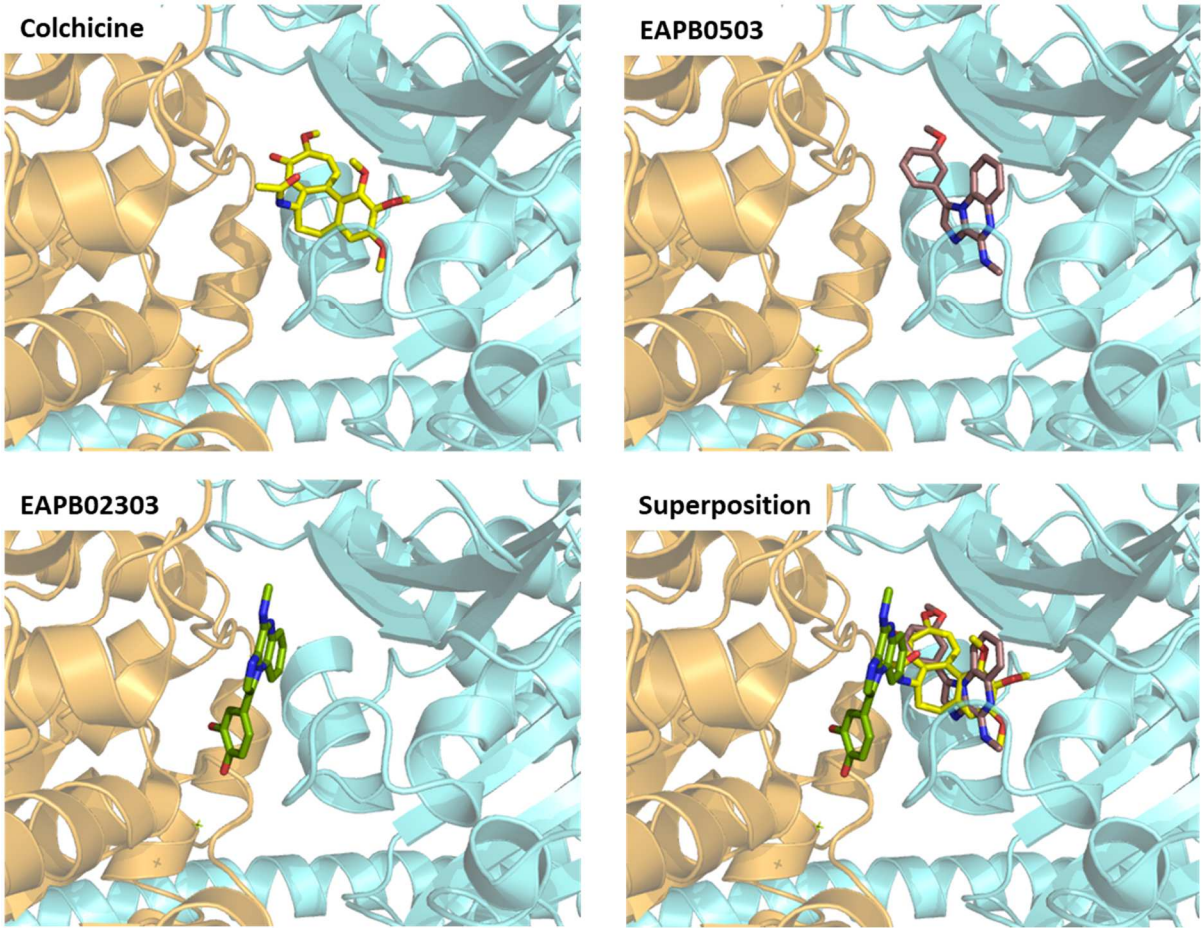

Figure 2: Docking studies. Compounds in the colchicine binding pocket of tubulin chains a and b (PDB 4O2B): Colchicine, EAPB0503, EAPB02303 (9d), EAPB02303 (9d) and colchicine overlay.

2.2. *In vitro* tubulin polymerization assay and first antiproliferative results

To investigate the results based on *in silico* molecular docking studies, we synthesized compound **EAPB02303** (**9d**) (see 2.3.) which is characterized by the presence of the 3,4-dihydroxyphenyl group on position 1 of the 4-methylaminoimidazo[1,2-*a*]quinoxaline heterocycle platform instead of the 3-methoxyphenyl group as in our first lead **EAPB0503**. As the mechanism of action of our hit **EAPB0503** was previously linked to its capability to inhibit tubulin polymerization,[31,32] we wanted to evaluate the capability of the new derivative **EAPB02303** for binding and inhibiting tubulin polymerization.

The results on tubulin polymerization are depicted on Figure 3. Tubulin was purified from pig brain tissue according the protocol described in Experimental Section (see 4.3.). A well-known natural tubulin inhibitor, colchicine, was used as reference. The previous reported data showed an important role of **EAPB0503** as antiproliferative and antimitotic agent, as **EAPB0503** (at 5 µM) was highly effective to inhibit tubulin assembly with 84% of inhibition, which is higher than colchicine (52% of inhibition ($P < 0.05$)). This high effect on tubulin inhibition was clearly correlated with its potent antiproliferative effect on human melanoma cell line. In the current study, it is clear that compound **EAPB02303** does not behave as our first hit **EAPB0503** as the profile for the new compound is the

same as vehicle DMSO. By this way, it was clear that **EAPB02303** was devoid of any inhibition on tubulin polymerization.

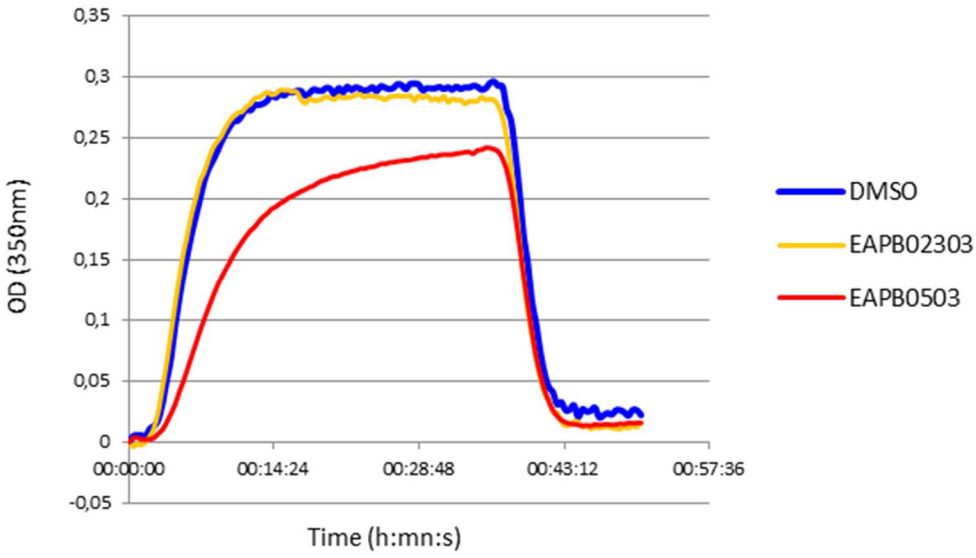

Figure 3: Tubulin polymerization inhibition.

Based on these results, it was highly interesting to determine if such dramatic loss of tubulin polymerization inhibition was detrimental to the anti-cancer activity of our Imiqualines series. **EAPB02303** was further tested on our A375 melanoma cell line model. Its IC_{50} found in the nanomolar range (3 nM) is much lower than the best results obtained with compounds of the Imiqualines first generation (*e.g.* 383 nM for **EAPB0503**). These results showed that the antiproliferative activity was highly impacted by the loss of tubulin inhibition, but the observed impact was in any case detrimental but, on the contrary, dramatically beneficial.

These very promising results prompted us to design derivatives of EAPB02303 with the catechol moiety and to synthesize two new series of imidazo[1,2-*a*]quinoxalines and imidazo[1,2-*a*]pyrazine derivatives with a catechol moiety directly linked to the imidazole ring.

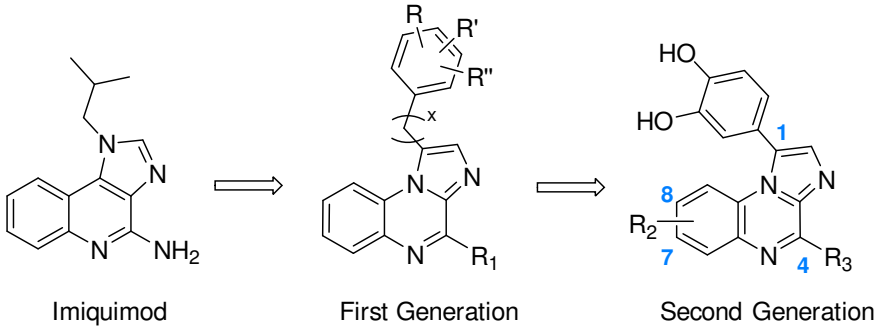

Scheme 1: Chemical structures of reference compound Imiquimod, first and second generations of Imiqualines.

2.3. Chemistry: synthesis of the novel Imiqualines generation

2.3.1. Imidazo[1,2-*a*]quinoxaline derivatives

Structural modifications on our imidazo[1,2-*a*]quinoxaline derivatives have been consequently done. Further to first impressive results obtained with compound **EAPB02303**, the second generation we designed is based on the 3,4-dihydroxyphenyl group on position 1. This substituent will not change during this study for the target imidazo[1,2-*a*]quinoxalines and imidazo[1,2-*a*]pyrazines. We present here a series of novel compounds with modifications on the one hand on the quinoxaline ring as methyl group was until today the only considered substituent, and on the other hand on position 4 by introducing small alkylamino or hydroxy groups.[34,35] Firstly, we worked on the screening of new substituents of the quinoxaline ring. The smallest alkylamine group on position 4, that is to say methylamine, remained. The trifluoromethyl and trifluoromethoxy derivatives were chosen among the commercially available *o*-fluoroanilines substituted on positions 7 or 8 to finally afford compounds **8a-8c** and **9a-9c**. Secondly, we modified the methylamine group on position 4 by introducing different kinds of alkyldiamine or alkoxy (**8j**, **9j**) moieties, remaining the quinoxaline devoided of any ring substituent. Among the commercially available monoprotected diamine, we chose the ethyl (**8e**, **9e**), propyl (**8f**, **9f**), hexyl (**8g**, **9g**) and piperazine (**8h**, **9h**) derivatives. The dimethylamine derivatives were obtained by using the corresponding nucleophilic amine (**8i**, **9i**).

From a chemical strategy point of view, the synthetic pathways of the imidazo[1,2-*a*]quinoxaline derivatives used in this study are given in schemes 2 and 3. Compounds were synthesized according to a route we previously partially described.[27,31,34,36] The carbonylimidazole dimer **2** results from the condensation of the 2-imidazole carboxylic acid **1** in presence of thionyl chloride.
Diversification of the quinoxaline ring was until today few explored by our team. We only considered mono- or dimethyl groups (R_2 substitution). Among the commercially available *o*-fluoroanilines, we chose the cyano, trifluoromethyl and trifluoromethoxy derivatives in position 4 or 5. Addition of *o*-fluoroaniline on the dimer **2** gives the intermediates **3a-3d**. The others commercially available reagents (methylcarboxylic acid and tert-butycarbamate) do not allow us to complete the synthetic pathway due to their sensitivity to acid and basic conditions used during the synthesis, leading to ester saponification and amino-deprotection, respectively. Moreover, the intermediates corresponding to the methylsulfonyl substituted *o*-fluoroaniline were never detected by mass spectrometry. Unfortunately, the *o*-fluoroanilines substituted in position 3 weren't suitable reagents, their lack of reactivity was probably due to their inductive and mesomeric effects on the fluoroaniline. The *o*-fluoroanilines substituted in position 6 were not investigated.
Cyclisation of **3a-3d** is allowed by using sodium hydride in dimethylacetamide to afford **4a**-**4d**. Treatment of compounds **4a**-**4d** with phosphorus oxychloride and *N,N*-diethylaniline gives the chlorinated compounds with a satisfactory yield for **5d**, lower for **5c** and very low for **5a** and **5b**. The use of phosphorus pentachloride as chlorinated agent and solvent[37] leads globally to lower yields (data not shown).
The chlorine of **5a**-**5d** is substituted by diverse nucleophilic groups under microwave assistance with good to excellent yields. To obtain the compounds **6a**-**6d**, methylamine is used in ethanol. The compounds **6e**-**6h** are obtained by addition of the corresponding monoprotected diamine in

presence of diisopropylethylamine in acetonitrile. Compound **6i** is obtained with the same procedure using dimethylamine as nucleophile. The preparation of compound **6j** required an adjustment. The use of sodium methanolate in methanol in the same microwave conditions used for the others lead exclusively to the hydroxy derivative, whereas the methoxy derivative could be furnished under reflux during 2 hours followed by a stirring overnight at room temperature.[38] Cherng *and al.* describe nucleophilic substitutions of halides on quinoline or isoquinoline structures under microwave irradiations.[39] The use of sodium methanolate in methanol under microwave irradiations at 70°C during 2 minutes leads to the desired compound **6j** with an excellent yield. Compound **6k** is obtained by using aqueous ammonia under microwave assistance at 130°C during 2 hours.

The bromination of intermediates **6a**-**6k** by *N*-bromosuccinimide in chloroform leads to compounds **7a**-**7k** quantitatively. The 3,4-dimethoxyphenyl moiety is introduced in position 1 of the imidazo[1,2-*a*]quinoxaline *via* a Suzuki-Miyaura cross-coupling reaction using the corresponding boronic acid to furnish compounds **8a**-**8k**. Optimal conditions correspond to the use of tetrakis(triphenylphosphine) palladium (0) with sodium carbonate in dimethoxyethane/water (2/1) under microwave irradiations at 140°C during 20 minutes.

Intermediates **8a**-**8k** are submitted to deprotection to afford the targeted compounds **9a**-**9k**. We previously used iodocyclohexane in dimethylformamide under microwave irradiations at 200°C during 1h20. Those conditions do not allow the cleavage of all the protections engaged in this synthetic pathway and afford generally low yields. Greene *and al.* described many methods for the cleavage of methyl ethers of phenols.[40] The more common conditions are based on bore derivatives as demethylating agents. Spadoni *and al.* use boron tribromide in dichloromethane.[41] These most described conditions in literature give good yields and are compatible with different kind of structures and chemical functions. Perspicace *and al.* use the complex BF_3-SMe_2 in presence or not of triethylamine in dichloromethane.[42,43] All these conditions were tested with some of our derivatives. Only boron tribromide in dichloromethane leads readily, with completion and cleanly to the targeted compounds **9a**-**9k.** Moreover, with these conditions, we observed that the Boc protective group is removed faster than the methyl protecting groups.

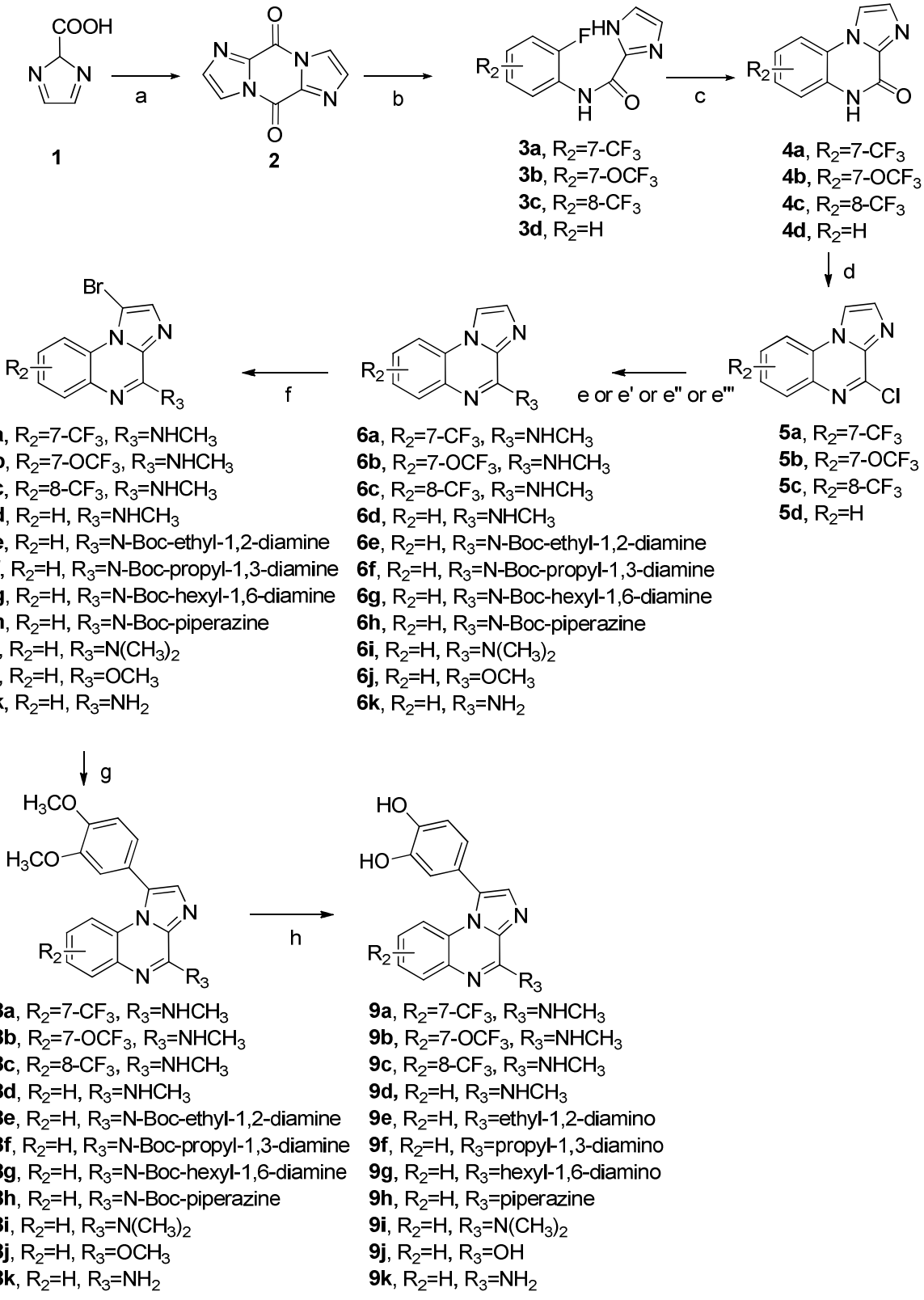

Scheme 2: General synthetic pathway to synthetize the targeted imidazo[1,2-*a*]quinoxalines 9a to 9k. Reagents and conditions : (a) $SOCl_2$, reflux, 24h; (b) corresponding *o*-fluoroaniline, NaHMDS, THF, 1h at 0°C then 3h at RT; (c) NaH, DMA, reflux, 48h; (d) N,N-DEA, $POCl_3$, MW (2 x 15 min, 130°C); (e) NH_2CH_3, EtOH, MW (20 min, 150°C); (e') RNH_2 (R ≠ CH_3) or $NH(CH_3)_2$, DIEA, ACN, MW (20 min, 150°C); (e'') MeONa, MeOH, MW (2 min, 70°C); (e''') NH_4OH, ACN, MW (2 h, 140°C); (f) NBS, $CHCl_3$, reflux, 1h30; (g) 3,4-dimethoxyphenylboronic acid, $Pd(PPh_3)_4$, Na_2CO_3, DME/H_2O (2/1), MW (20 min, 140°C); (h) BBr_3, CH_2Cl_2, 0°C to RT, 3h.

Two of our target compounds **9e** and **9g** were converted in ammonium chloride salts **10e** and **10g** by using hydrochloric acid in dioxane (4M) (Scheme 3).

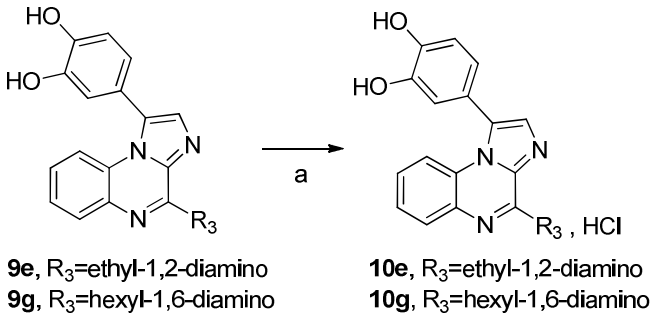

9e, R_3=ethyl-1,2-diamino
9g, R_3=hexyl-1,6-diamino

10e, R_3=ethyl-1,2-diamino
10g, R_3=hexyl-1,6-diamino

Scheme 3: Synthetic pathway for ammonium chloride salts preparation. Reagents and conditions: (a) HCl/dioxane (4M), 2h, RT.

2.3.2. Imidazo[1,2-*a*]pyrazine derivatives

In parallel of the synthesis of the imidazo[1,2-*a*]quinoxaline derivatives, we also designed a series of imidazo[1,2-*a*]pyrazines to evaluate the potency of this minimal structure. Several synthetic pathways to obtain imidazo[1,2-*a*]pyrazine derivatives have been described in the literature.[44–46] We chose to focus on the following one we previously described (Scheme 4)[34], because of the diverse substituents we wanted to graft on positions 1 and 4.[47] Starting material 3-bromo-8-chloroimidazo[1,2-*a*]pyrazine is commercially available. Methylamine or ammoniac is first introduced in position 4 under microwave assistance without shifting the bromine to obtain compounds **11a** or **11b**, respectively. The 3,4-dimethoxyphenyl group is then introduced by the Suzuki-Miyaura cross-coupling reaction with the appropriate aryl boronic acid in presence of carbonate salt and palladium catalyst under microwave irradiations to furnish compounds **12a** and **12b**. A deprotecting step is engaged with boron tribromide in dichloromethane to regenerate the hydroxyl groups on the aryl moiety to afford **13a** and **13b**.

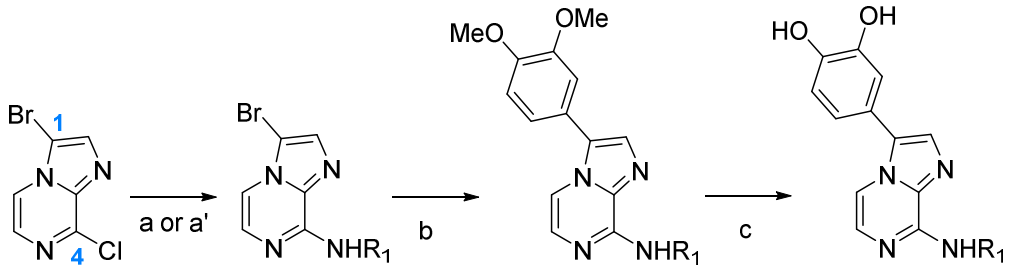

11a: R_1=CH_3
11b: R_1=H

12a: R_1=CH_3
12b: R_1=H

13a: R_1=CH_3
13b: R_1=H

Scheme 4: Synthesis of imidazo[1,2-*a*]pyrazine derivatives. Reagents and conditions: (a) NH_4OH, ACN, MW (2h, 130°C); (a') CH_3NH_2, EtOH, MW (20 min, 140°C) ; (b) 3,4-dimethoxyphenylboronic acid, Na_2CO_3, $Pd(PPh_3)_4$, DME/H_2O (1/1), MW (20 min, 140°C) ; (c) BBr_3, CH_2Cl_2, 0°C to RT, 2h.

2.4. *In vitro* cell growth inhibition assay

We have evaluated the cellular activity of compounds **6d**, **7d**, **8b**-**8j**, **9a**-**9k**, **10e**, **12a**-**12b**, **13a**-**13b** to investigate their efficacy on the A375 human melanoma cell line proliferation, which

possesses the BRAF mutation. Results are reported in Table 1 and compared to the positive control vemurafenib, used as targeted therapy of BRAF mutant melanoma.

The analysis of the structure-activity relationship confirms the interest of small alkylamino groups (such as methylamine, dimethylamine or amine) in position 4 as depicted by compounds **8d**, **8i**, **9d, 9i** and **9k**, compared to vemurafenib. Nor longer chains as ethyl (**8e** and **9e**), propyl (**8f** and **9f**), hexyl (**8g** and **9g**) or cyclic alkylamine chain as piperazine (**8h** and **9h**), nor the hydrochlorine salt of the ethyl derivative **10e** improve the cytotoxic activities. Even if compound **8j** bearing a methoxy group in position 4 displays a micromolar activity, its demethylated analogue **9j** completely loses the cytotoxic activity. Moreover, substitutions of the quinoxaline ring by the trifluoromethyl or trifluoromethoxy group are tolerated on position 7 (**8b**, **9a**, **9b**) , which is not the case in position 8 (**8c** and **9c**). Their synthetic intermediates **6d** and **7d** do not display better in vitro activity, confirming the interest of the catechol moiety. The *in vitro* results highlight the necessity of the entire aromatic structure for antiproliferative activity, that is to say the hetero-tricyclic nucleus of the imidazo[1,2-a]quinoxaline, since the IC_{50} values of the four prepared imidazo[1,2-a]pyrazines **12a-b** and **13a-b** are above 10 µM. These results allowed us to highlight compounds **EAPB02303** (**9d**) and its *N*-demethylated derivative **EAPB02302** (**9k**) as very active leads of the second Imiqualine generation, with ICs50 of 3 and 60 nM respectively. Additional modifications did not contribute to improve the anti-proliferative activity, since the compounds show micromolar activities similar to those of our first Imiqualine series.

Table 1 : IC_{50} values on human melanoma A375 cell line.

Compounds		IC_{50} (nM)
vemurafenib		139
6d		>10000
7d		2354
8b	**EAPB02203-7b**	3493
8c	**EAPB02203-8a**	>10000
8d	**EAPB02203**	193
8e	**EAPB02211**	>10000
8f	**EAPB02214**	>10000
8g	**EAPB02212**	>10000
8h	**EAPB02213**	>10000
8i	**EAPB02204**	414
8j	**EAPB02215**	2929
9a	**EAPB02303-7a**	6909
9b	**EAPB02303-7b**	199
9c	**EAPB02303-8a**	>10000
9d	**EAPB02303**	3
9e	**EAPB02306**	1284
9f	**EAPB02309**	5588
9g	**EAPB02307**	5694
9h	**EAPB02308**	>10000
9i	**EAPB02304**	30
9j	**EAPB02300**	> 10 000
9k	**EAPB02302**	60

10e	**EAPB02306s**	1704
12a	**EAPB32203**	> 10 000
12b	**EAPB32202**	> 10 000
13a	**EAPB32303**	> 10 000
13b	**EAPB32302**	> 10 000

Considering the astonishing activity of **EAPB02303**, we evaluated its potential on different melanoma cell lines (A375, ME WO, A2058, IPC 298), compared to our first generation hit **EAPB0503** and vemurafenib (Figure 3 and Table 2). Whereas vemurafenib selectively inhibits BRAF v600e melanoma cell lines, our compound **EAPB02303** is able at a nanomolar range to inhibit growth of all melanoma cell lines tested in this assay. It is interesting to note that EAPB02303 does not exhibit any cytotoxicity on freshly isolated hPBMCs at concentrations as high as 0.2 mM. Those *in vitro* data prompt us to only considered **EAPB02303** for the rest of the entire study to start an in-depth research of the biological target(s) and/or mechanism of action.

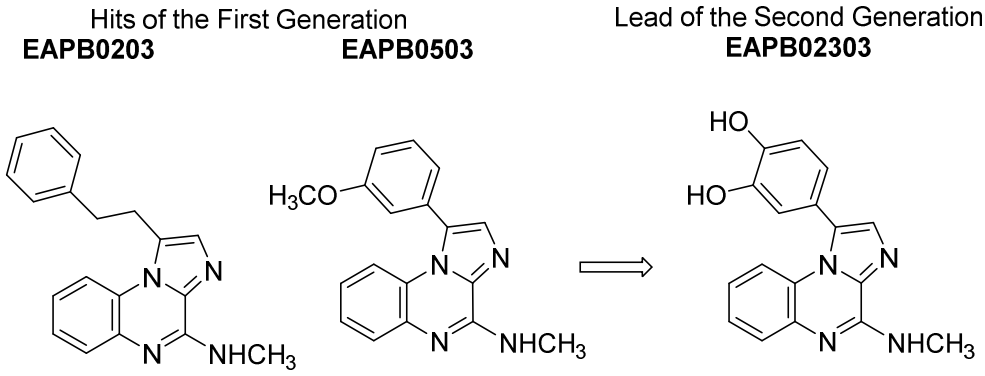

Figure 3: Chemical structures of first and second Imiqualines generations

Table 2: IC50 values of EAPB02303 and EAPB0503 on different melanoma cell lines compared to vemurafenib

Cell lines	IC_{50} (nM)			BRAF mutation
	EAPB02303	EAPB0503	vemurafenib	
A375	3	383	139	v600e
ME WO	3	125	283[50]	-
A2058	4	185	425[50]	v600e
IPC 298	40	469	13000[51]	-

2.5. Transcriptomic data

The mode of action of treatments on cancer cells can be correlated with the modification of their transcriptomes. To precise the mechanism of action of our Imiqualines family, we designed a transcriptomic study to carry out a comparison with different therapies used in human cancer treatment. Thus, **EAPB0203, EAPB0503** and **EAPB02303** were compared to a panel of 12 drugs, which are representative of the diversity of anticancer mechanisms of action. Among them, 11 conventional chemotherapies belonging to different therapeutic classes were selected. The alkylating agents were represented by dacarbazine (reference molecule for Multiple Myeloma (MM) treatment

until 2011) and fotemustine (also used in MM treatment in case of brain metastases). The anti-metabolites were represented by 5-fluorouracil (5-FU, antipyrimidine) and methotrexate (folic acid antagonist). SN38 (the active metabolite of irinotecan) and Doxorubicin were chosen as topoisomerase inhibitors (topoisomerases I and II respectively). Finally, we included vemurafenib (BRAF inhibitor) as targeted therapy. Moreover, as the first generations of Imiqualines (**EAPB0203** and **EAPB0503**) conserved the anti-microtubule activity of imiquimod[31], imiquimod and a panel of molecules with anti-tubulin activities were also included in the study. These drugs fix different "binding sites" of tubulin: vinca-alkaloid binding site (vinorelbine), taxane binding site (paclitaxel), colchicine binding site (colchicine), and maytansine binding site (maytansine). **EAPB02303** was compared to all these mentioned drugs.

From an experimental point of view, A375 cells were treated for 6 hours by each drug at a concentration of 10 µM. Then, the transcriptome of treated or non-treated cells (DMSO was used as negative control) was established after hybridization on Affymetrix HG U133 + PM genechip. The experiment aimed to characterize the genes whose level of transcription was disturbed following the application of the different studied drugs. The analysis of transcription profiles allowed the calculation of a distance between all the drugs taken two by two. These distances were converted into a dendrogram which is represented here by the synthetic form of a tree (Figure 5).

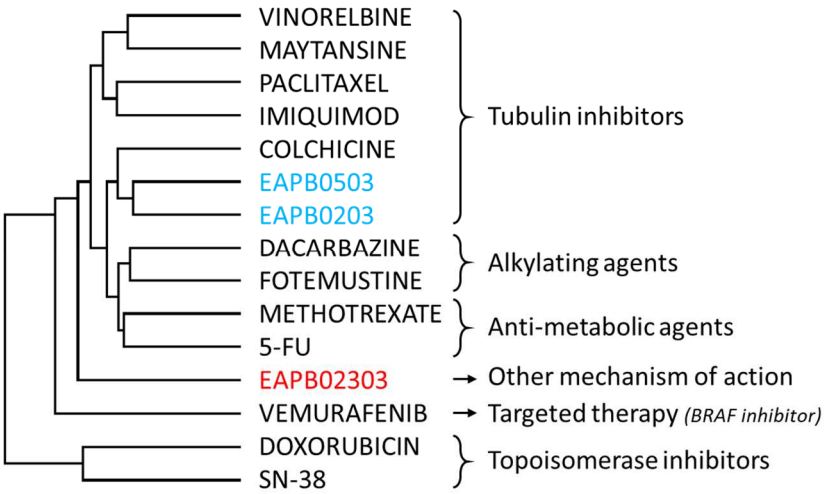

Figure 5: Dendrogram of transcriptomic profiles. Comparison of gene expression profiles of A375 cells after a treatment with Imiqualines derivatives (EAPB0203, EPAB0503, EAPB02303), or a panel of anticancer drugs (6h, 10 µM). The distances between each pair of cell lines were calculated as described in materials and methods and represented as a dendrogram of distances.

In this Figure 5, we can observe that molecules sharing a common mechanism of action are grouped, which give a good confidence in the obtained results. Two of the three tested Imiqualines derivatives, **EAPB0203** and **EAPB0503** (Figure 1), are included among anti-tubulin agents. This set is itself split into two groups, one of these consisting in **EAPB0203**, **EAPB0503** and colchicine. This notable result confirms both the anti-tubulin component of their mechanism of action, and the probably binding on the colchicine site.[31] In addition, **EAPB02303** is clearly set apart from all anti-tubulin agents, confirming the loss of the anti-tubulin component in its mechanism of action. Moreover, and very interestingly, **EAPB02303** is not associated with any group. Thus, its mechanism of action appears to significantly differ from other first generation Imiqualines derivatives, but also from those of the other tested drugs. A finer and targeted analysis of these transcriptomic data could allow to better understand the original mechanism of action of **EAPB02303** in highlighting cellular or

molecular signaling pathways, that are recruited or inhibited. A screening over 450 kinases could not allow us to put forward any enzyme inhibition. Furthermore, chemical biology studies including SILAC method will allow us to refine and precise biological targets.

2.6. In vivo study

To test the efficacy of the **EAPB02303** to inhibit tumor growth in a heterotopic xenograft mouse model of human melanoma, we inoculated subcutaneously A375 cells to immunodeficient mice and treated the animals by intraperitoneal injection of the compound as soon as the tumors reached a minimal volume.

At the maximum tolerated dose (75 mg/kg - 2 times a week), **EAPB02303** treatment induced a significant reduction in the tumor size, around 80% smaller as compared to the vehicle group (Figure 6A). However severe adverse side effects were observed such as significant reduction in body weight, morbidity and mortality (Figure 6B and data not shown). Gross pathology findings at study termination revealed pathological findings mainly on the liver, spleen, gut and pancreas. (Supplementary Table S1).

Interestingly, by giving the same dose level per week (150 mg/kg) but by changing the dose regimen (5 times a week), the compound had the same efficacy on tumor size without apparent toxicity. No significant impact on body weight, neither side effects were observed (Figures 6A and 6B). This clinical observation was supported by gross pathology analysis at study termination (data not shown). For treatment at 25 mg/kg – 3 times a week, the reduction of tumor size was found to be 50%, which suggest a dose-dependent response (Figure 6A). Finally, for all regimen, tumor weight measurements at necropsy showed a similar pattern to the calculated tumor size (Figures 6C and 6D).

Histologic analyses, as displayed in supplementary Table S2, show **EAPB02303** did not induce changes regarding tumor stroma, inflammation and vascularization. Tumors blood flow or indicative angiogenic parameters were not modified in comparison to the vehicle group as indicated by Laser Doppler measurements (data not shown). It was observed a marked trend toward a lower invasion in group 30 mg/kg – 5 times a week, a moderately low trend to invade in group 25 mg/kg – 3 times a week, intermediate invasion in group 75 mg/kg – 2 times a week and a higher trend toward invasion in vehicle group.

EAPB02303 also induced a trend toward a decreased curve of the mitotic index. In the groups 75 mg/kg – 2 times a week and 25 mg/kg – 3 times a week, the number of mitosis was lower than in the vehicle group (Figures 6E and 6F). Moreover, the mitotic index was even below in group 30 mg/kg – 5 times a week.

To summarize, **EAPB02303** exerted *in vivo* an anti-cancer effect that was highly correlated with a low mitotic index and a lower invasion capacity correlate but not with an anti-angiogenic nor necrotic activity. Therefore, the efficacy of this compound is probably linked to an effect involving mitosis. **EAPB02303** compound, at the highest dose and when administered 2 times a week, was coupled to a significant toxicity. By changing the dose regimen with the same dose level per week (150 mg/kg), same efficacy was achieved without apparent toxicity indicating that **EAPB02303** toxicity might relate to C_{max} but not its efficacy.

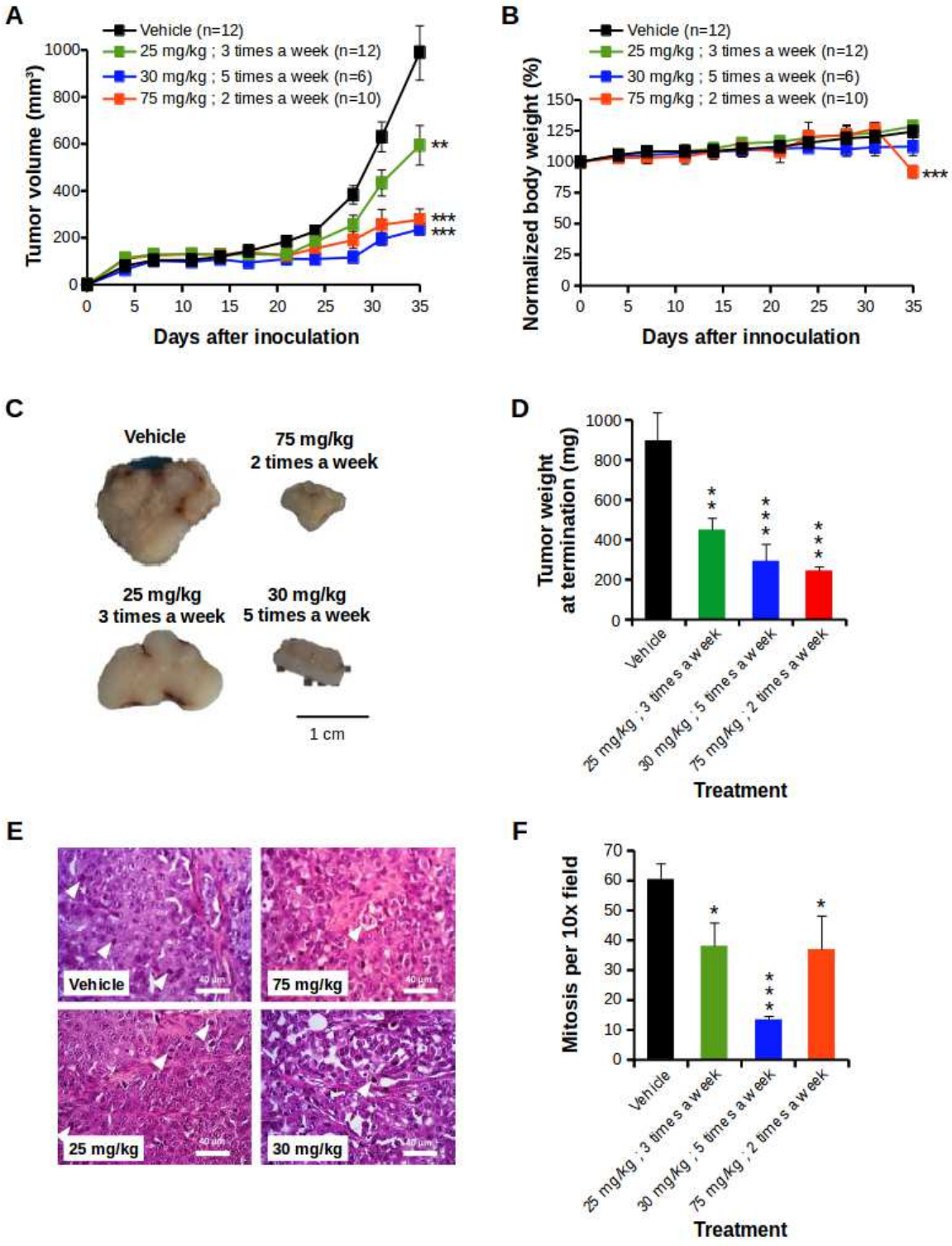

Figure 6: Tumorigenesis experiment with subcutaneously inoculated A375 melanoma cells in animals treated with indicated regimen of EAPB02303. EAPB02303 treatment inhibits tumor growth in heterotopic xenograft mouse model. A: Growth kinetics of tumors in animals treated with the indicated regimen (number of independent transplants is indicated in the figure). B: Averages of normalized body weight of tumor-bearing animals during treatment with the indicated regimen. C: Representative macroscopic pictures of tumors after mid-sagittal section from indicated mice. D: Weight of tumors after necroscopy of the indicated mice. E: Representative hematoxylin/eosin/saffron-stained samples from tumors of the indicated mice (scale bar, 40 µm). F: Quantification of mitosis from the indicated mice. n = 4 mice for each group. Data are presented as mean ± s.e.m. * p<0.05; ** p<0.01; *** p<0.001 relative to values obtained by vehicle-treated animals.

3. Conclusion

Imiqualines first generation exhibited *in vitro* antiproliferative effects on melanoma cell lines and high tubulin inhibitory effects. As tubulin inhibition is not specific of cancer cells, molecular docking studies drove us to the synthesis of new compounds with a catechol moiety directly linked to the imidazole ring of the tricyclic heterocycle scaffold. Structural modifications of the first hits, **EAPB0203** and **EAPB0503**, afforded two new leads, **EAPB02303** (**9d**) and its *N*-demethylated derivative **EAPB02302** (**9k**), with utmost impressive *in vitro* activities on A375 human melanoma cancer cell line in the nanomolar range with a loss of tubulin polymerization for EAPB02303. The transcriptomic analysis further demonstrated that the mechanism of action for **EAPB02303** is clearly different from a panel of well-known anticancer drugs, attesting the novelty and originality of its mechanism of action. *In vivo* **EAPB02303** treatment reduced tumor size and weight of the A375 human melanoma xenografts in a dose-dependent manner, correlated with a low mitotic index but not with necrosis. The patented compound **EAPB02303** is today under preclinical studies and further on-going studies are implemented to determine the molecular target(s) and to precise the mechanism of action of Imiqualines second generation.

4. Materials and Methods

4.1. Chemistry

4.1.1. General

All solvents and reagents were obtained from Sigma Aldrich Chemical Co., Iris Biotech GmbH, Alfa Aesar Co, VWR and FluoroChem UK and used without further purification unless indicated otherwise. Silica gel chromatography was conducted with 230-400 mesh 60 Å silica gel (Sigma Aldrich Chemical Co.). Thin layer chromatography plates (Kieselgel 60 F254) were purchased from Merck. The progress of reaction was monitored by TLC exposure to UV light (254 nm and 366 nm). Microwave assisted organic syntheses were performed on the Biotage Initiator 2.0 Microwave. ^{1}H and ^{13}C NMR spectra were obtained on Brüker AC-400 spectrometer (Laboratoires de Mesures Physiques, Plateau technique de l'Institut des Biomolécules Max Mousseron, Université de Montpellier, Montpellier, France). Chemical shifts are given as parts per million (ppm) using residual dimethylsulfoxide signal for protons (δ_{DMSO} = 2.46 ppm) and carbons (δ_{DMSO} = 40.00 ppm). Abbreviations used for signal patterns are the following: s, singlet; d, doublet; t, triplet; q, quartet; m, multiplet. Coupling constants are reported in Hertz (Hz). Mass spectral data were obtained on a Micromass Q-Tof (Waters) spectrometer equipped with ESI source (Laboratoires de Mesures Physiques, Plateau technique de l'Institut des Biomolécules Max Mousseron, Université de Montpellier, Montpellier, France). Mass spectra were recorded in positive mode between 50 and 1500 Da, capillary and cone tension were 3000 and 20 V, respectively. The High Resolution Mass Spectroscopy (HRMS) analyses are carried out by direct introduction on a Synapt G2-S mass spectrometer (Waters, SN: UEB205) equipped with ESI source (Laboratoires de Mesures Physiques, Plateau technique de l'Institut des Biomolécules Max Mousseron, Université de Montpellier, Montpellier, France). The mass spectra were recorded in positive mode, between 100 and 1500 Da. The capillary tension is 3000 V and the cone tension is 30 V. The source and desolvation temperature are 120°C and 250°C, respectively.

Compounds **2, 3d, imidazo[1,2-*a*]quinoxalines 4d, 5d, 6d, 7d, and imidazo[1,2-*a*]pyrazines 11a-b, 12a-b** and **13a-b** were prepared as previously described in literature.[27,31,34,36]

4.1.2. General procedure for the addition of the fluoroaniline.

To 2-fluoroaniline (56.5 mmol) in THF (28 mL) cooled in a -10°C bath, sodium bis(trimethylsilyl)amide (141 mmol, 1.0 M in THF) was added. After stirring for 1 hour, a suspension of **2** (25.6 mmol) in THF (30 mL) was added. The mixture was allowed to warm to room temperature and stirred for 3 hours. Acetic acid was carefully added to obtain pH 7. The reaction mixture was concentrated under vacuum, followed by the addition of water and saturated aqueous $NaHCO_3$ solution (v/v, 1/1, 100 mL). The solid was collected by filtration, washed with distilled water and cyclohexane until red-color disappearance, and dried under vacuum. The compound **3** is obtained as a solid and used without further purification.

4.1.3. General procedure for the cyclisation.

To **3** (20 mmol) in dimethylacetamide (160 mL) was carefully added and sodium hydride (30 mmol). The reaction mixture was heated to reflux for 24 hours. After being cooled, a second portion of sodium hydride (30 mmol) was added and the reaction mixture was heated to reflux during 24 hours. The sodium hydride was neutralized with saturated aqueous NH_4Cl solution (40 mL) and the reaction mixture was then concentrated under vacuum. The residue was suspended in water, filtered, washed with water. The precipitate **4** was dried under vacuum and used without further purification.

4.1.4. General procedure for the chlorination.

Phosphorus oxychloride (60.2 mmol) and *N,N*-diethylaniline (5.72 mmol) were added to **4** (2.86 mmol) in a microwave-adapted vial and sealed. The reaction was submitted to microwave irradiations at 130°C for 15 min. The reaction mixture was carefully poured dropwise in a saturated aqueous Na_2CO_3 solution (50 mL) to be neutralized. When effervescence stopped, the solution was extracted with dichloromethane (3x50 mL). The organic layer was dried over $MgSO_4$, filtered and concentrated under reduced pressure. The crude mixture was purified by flash chromatography eluted with cyclohexane/ethyl acetate to afford compound **5**.

*4-chloro-7-(trifluoromethyl)imidazo[1,2-a]quinoxaline (**5a**).* Yield: 7%. $C_{11}H_5ClF_3N_3$. Mw: 271.63 g/mol. Mp: 139°C. ^{1}H-NMR δ (ppm, 400 MHz, DMSO d_6) 7.97 (s, 1H, CH 2), 8.15 (d, 1H, CH 8, *J=8Hz*), 8.39 (s, 1H, CH 6), 8.67 (d, 1H, CH 9, *J=8Hz*), 9.08 (s, 1H, CH 1). ^{13}C-NMR δ (ppm, 100 MHz, DMSO d_6) 117.97 (CH 1), 118.32 (CH 9), 126.03 (CH 8), 126.77 (CH 6), 127.63 and 127.96 (Cq 7, CF_3), 130.23 (Cq 5a), 134.40 (Cq 3a), 135.37 (CH 2), 136.12 (Cq 9a), 144.42 (Cq 4). ^{19}F-RMN δ (ppm, 376.5 MHz, DMSO d6) -60.47. MS (ESI +, QTof, m/z): 272.10 $[M+H]^+$

*4-chloro-7-(trifluoromethoxy)imidazo[1,2-a]quinoxaline (**5b**).* Yield: 34%. $C_{11}H_5ClF_3N_3O$. Mw: 287.63 g/mol. Mp: 176°C. ^{1}H-NMR δ (ppm, 400 MHz, DMSO d_6) 7.84 (d, 1H, CH 8, *J=8Hz*), 7.93 (d, 1H, CH 2, *J=4Hz*), 8.02 (s, 1H, CH 6), 8.56 (d, 1H, CH 9, *J=8Hz*), 9.01 (d, 1H, CH 1, *J=4Hz*). ^{13}C-NMR δ (ppm, 100 MHz, DMSO d_6) 117.75 (CH 1), 118.69 (CH 9), 121.26 (CH 6), 122.98 (CH 8), 126.75 (Cq 5a), 135.19 (CH 2), 135.29 (Cq 3a), 135.75 (Cq 9a), 144.30 (Cq 4), 146.60 and 146.62 (Cq 7, OCF_3). ^{19}F-RMN δ (ppm, 376.5 MHz, DMSO d6) -57.47. MS (ESI +, QTof, m/z): 287.90 $[M+H]^+$

*4-chloro-8-(trifluoromethyl)imidazo[1,2-a]quinoxaline (**5c**).* Yield: 12%. $C_{11}H_5ClF_3N_3$. Mw: 271.63 g/mol. Mp: 155°C. ^{1}H-NMR δ (ppm, 400 MHz, DMSO d_6) 7.96 (s, 1H, CH 2), 8.00 (d, 1H, CH 7, *J=8Hz*), 8.19 (d, 1H, CH 6, *J=8Hz*), 8.94 (s, 1H, CH 9), 9.18 (s, 1H, CH 1). ^{13}C-NMR δ (ppm, 100 MHz, DMSO d_6) 114.92 (CH 9), 118.20 (CH 1), 123.68 (CH 7), 125.01 (CF_3), 127.86 (CH 6), 129.16 (Cq 8), 129.87 (Cq 5a), 130.69 (CH 2), 135.94 (Cq 3a), 136.93 (Cq 9a), 145.22 (Cq 4). ^{19}F-RMN δ (ppm, 376.5 MHz, DMSO d6) -60.32. MS (ESI +, QTof, m/z): 271.80 $[M+H]^+$

4.1.5. General procedure for the introduction of the methylamino group.

A 33% (w/v) ethanol solution of methylamine (49.0 mmol) was added to a solution of **5** (2.45 mmol) in ethanol (7 mL) in a microwave-adapted vial. The reaction was submitted to microwave irradiations during 20 minutes at 150°C. The solvent was removed under reduced pressure. The crude mixture was dissolved in ethyl acetate and successively washed with saturated aqueous chloride ammonium, distilled water and finally brine. The organic layer was dried on sodium sulphate, filtered and concentrated under reduced pressure. The crude mixture was purified by flash chromatography eluted with cyclohexane/ethyl acetate to afford compounds **6a-6d** as solids.

*N-methyl-7-(trifluoromethyl)imidazo[1,2-a]quinoxalin-4-amine (**6a**).* Yield: 94%. $C_{12}H_9F_3N_4$. Mw: 266.22 g/mol. Mp: 225°C. ^{1}H-NMR δ (ppm, 400 MHz, DMSO d_6) 3.04 (d, 3H, *CH*$_3$NH, *J=8Hz*), 7.60 (d, 1H, CH 8, *J=8Hz*), 7.67 (d, 1H, CH 2, *J=4Hz*), 7.85 (s, 1H, CH 6), 8.06 (d, 1H, *NH*CH_3, *J=4Hz*), 8.31 (d, 1H, CH 9, *J=8Hz*), 8.69 (d, 1H, CH 1, *J=4Hz*). ^{13}C-NMR δ (ppm, 100 MHz, DMSO d_6) 27.73 (CH_3NH), 115.71 (CH 1), 117.15 (CH 9), 118.92 (CH 8), 123.22 (CH 6), 127.10 to 127.42 (CF_3, Cq 7, Cq 5a), 132.76 (CH 2), 132.87 (Cq 3a), 137.63 (Cq 9a), 149.11 (Cq 4). ^{19}F-RMN δ (ppm, 376.5 MHz, DMSO d6) -60.42. MS (ESI +, QTof, m/z): 267.10 $[M+H]^+$

*N-methyl-7-(trifluoromethoxy)imidazo[1,2-a]quinoxalin-4-amine (**6b**).* Yield: 70%. $C_{12}H_9F_3N_4O$. Mw: 282.22 g/mol. Mp: 189°C. ^{1}H-NMR δ (ppm, 400 MHz, DMSO d_6) 3.04 (d, 3H, *CH*$_3$NH, *J=8Hz*), 7.28 (d, 1H, CH 8, *J=8Hz*), 7.49 (s, 1H, CH 6), 7.64 (d, 1H, CH 2, *J=4Hz*), 8.02 (d, 1H, *NH*CH_3, *J=4Hz*), 8.21 (d, 1H, CH 9, *J=8Hz*), 8.62 (d, 1H, CH 1, *J=4Hz*). ^{13}C-NMR δ (ppm, 100 MHz, DMSO d_6) 27.73 (*CH*$_3$NH), 115.51 (CH 1, CH 8), 117.49 (CH 9), 117.99 (CH 6), 123.79 (Cq 5a), 132.51 (CH 2), 132.84 (Cq 3a), 138.75 (Cq 9a), 146.69 and 146.71 (OCF_3, Cq 7), 149.06 (Cq 4). ^{19}F-RMN δ (ppm, 376.5 MHz, DMSO d6) -56.81 (OCF_3). MS (ESI +, QTof, m/z): 282.9 $[M+H]^+$

*N-methyl-8-(trifluoromethyl)imidazo[1,2-a]quinoxalin-4-amine (**6c**).* Yield: 82%. $C_{12}H_9F_3N_4$. Mw: 266.22 g/mol. Mp: 196°C. ^{1}H-NMR δ (ppm, 400 MHz, DMSO d_6) 3.06 (d, 3H, *CH*$_3$NH, *J=4Hz*), 7.65 (d, 1H, CH 2, 4Hz), 7.67 (d, 1H, CH 7, *J=8Hz*), 7.72 (d, 1H, CH 6, *J=8Hz*), 8.15 (m, 1H, NH), 8.55 (s, 1H, CH 9), 8.81 (s, 1H, CH 1). ^{13}C-NMR δ (ppm, 100 MHz, DMSO d_6) 27.75 (CH_3NH), 113.72 (CH 9), 115.88 (CH 1), 123.06 and 123.09 (CF_3, CH 7), 124.64 (Cq 5a), 126.28 (Cq 8), 127.08 (CH 6), 132.57 (CH 2), 132.95 (Cq 3a), 140.53 (Cq 9a), 149.49 (Cq 4). ^{19}F-RMN δ (ppm, 376.5 MHz, DMSO d6) -59.36 (CF_3). MS (ESI +, QTof, m/z): 267.00 $[M+H]^+$

4.1.6. General procedure for the introduction of an alkyldiamino group.

N-Boc-diaminoalkyl (3.69 mmol) and DIEA (4.9 mmol) were added to **5** (2.45 mmol) in acetonitrile (10 mL) in a microwave-adapted vial and sealed. The reaction was submitted to microwave irradiations at 150°C for 20 min and then evaporated. The residue was dissolved in ethyl acetate, washed with saturated ammonium chloride solution, water and brine. The organic layer was dried over $MgSO_4$,

filtered and concentrated under reduced pressure. Compound **6i** is obtained as a solid and used without further purification. The crudes mixtures were purified by flash chromatography eluted with cyclohexane/ethyl acetate to afford compounds **6e, 6f, 6g, 6h**.

*tert-butyl (2-(imidazo[1,2-a]quinoxalin-4-ylamino)ethyl)carbamate (**6e**).* Yield: 81%. $C_{17}H_{21}N_5O_2$. Mw: 327.38 g/mol. Mp: 135°C. ^{1}H-NMR δ (ppm, 400 MHz, DMSO d_6) 1.36 (s, 9H, 3 x CH_3 tBu), 3.26 (qd, 2H, *CH_2*NHBoc, *J=4Hz*), 3.61 (qd, 2H, *CH_2*NH, *J=4Hz*), 7.01 (t, 1H, *NH*Boc, *J=4Hz*), 7.28 (t, 1H, CH 7, *J=8Hz*), 7.30 (t, 1H, CH 8, *J=8Hz*), 7.58 (d, 1H, CH 9, *J=8Hz*), 7.62 (d, 1H, CH 2, *J=4Hz*), 7.68 (t, 1H, NH, *J=4Hz*), 8.11 (d, 1H, CH 6, *J=8Hz*), 8.60 (d, 1H, CH 1, *J=4Hz*). ^{13}C-NMR δ (ppm, 100 MHz, DMSO d_6) 28.68 (CH_3 tBu), 40.00 (*CH_2*NHBoc, *CH_2*NH), 78.07 (Cq tBu), 115.03 (CH 1), 115.83 (CH 6), 123.17 (CH 7), 124.77 (Cq 5a), 126.62 (CH 9), 126.78 (CH 8), 132.26 (CH 2), 132.45 (Cq 3a), 137.17 (Cq 9a), 147.79 (Cq 4), 156.23 (C=O carbamate). MS (ESI +, QTof, m/z): 328.18 $[M+H]^+$

*tert-butyl (3-(imidazo[1,2-a]quinoxalin-4-ylamino)propyl)carbamate (**6f**).* Yield: 93%. $C_{18}H_{23}N_5O_2$. Mw: 341.41 g/mol. Mp: 152°C. ^{1}H-NMR δ (ppm, 400 MHz, DMSO d_6) 1.37 (s, 9H, 3 x CH_3 tBu), 1.74 (m, 2H, *CH_2CH_2*NHBoc), 3.02 (qd, 2H, *CH_2*NHBoc, *J=4Hz*), 3.56 (qd, 2H, *CH_2*NH, *J=4Hz*), 6.93 (t, 1H, *NH*Boc, *J=4Hz*), 7.26 (t, 1H, CH 7, *J=8Hz*), 7.37 (t, 1H, CH 8, *J=8Hz*), 7.58 (d, 1H, CH 9, *J=8Hz*), 7.60 (s, 1H, CH 2, *J=4Hz*), 7.70 (t, 1H, NH, *J=4Hz*), 8.08 (d, 1H, CH 6, *J=8Hz*), 8.59 (s, 1H, CH 1, *J=4Hz*). ^{13}C-NMR δ (ppm, 100 MHz, DMSO d_6) 28.72 (CH_3 tBu), 29.77 (*CH_2CH_2*NHBoc), 37.76 (CH_2NH), 37.94 (*CH_2*NHBoc), 77.92 (Cq tBu), 115.04 (CH 1), 115.83 (CH 6), 123.03 (CH 7), 124.70 (Cq 5a), 126.50 (CH 9), 126.76 (CH 8), 132.23 (CH 2), 132.53 (Cq 3a), 137.26 (Cq 9a), 147.79 (Cq 4), 156.11 (C=O carbamate). MS (ESI +, QTof, m/z): 342.19 $[M+H]^+$

*tert-butyl (6-(imidazo[1,2-a]quinoxalin-4-ylamino)hexyl)carbamate (**6g**).* Yield: 89%. $C_{21}H_{29}N_5O_2$. Mw: 383.49 g/mol. Mp: 118°C. ^{1}H-NMR δ (ppm, 400 MHz, DMSO d_6) 1.29 to 1.40 (m, 15H, 3 x CH_3 tBu, *$CH_2CH_2CH_2$*NH, *$CH_2CH_2CH_2$*NHBoc, *CH_2CH_2*NHBoc), 1.64 (qt, 2H, *CH_2CH_2*NH, *J=8Hz*), 2.91 (qd, 2H, *CH_2*NHBoc, *J=4Hz*), 3.56 (qd, 2H, *CH_2*NH, *J=4Hz*), 6.76 (t, 1H, *NH*Boc, *J=4Hz*), 7.27 (t, 1H, CH 7, *J=8Hz*), 7.37 (t, 1H, CH 8, *J=8Hz*), 7.57 (d, 1H, CH 9, *J=8Hz*), 7.61 (d, 1H, CH 2, *J=4Hz*), 7.68 (t, 1H, NH, *J=4Hz*), 8.07 (d, 1H, CH 6, *J=8Hz*), 8.58 (d, 1H, CH 1, *J=4Hz*). ^{13}C-NMR δ (ppm, 100 MHz, DMSO d_6) 26.55 and 26.73 (*$CH_2CH_2CH_2$*NH, *$CH_2CH_2CH_2$*NHBoc), 28.73 (CH_3 tBu), 29.24 (*CH_2CH_2*NH), 29.95 (*CH_2CH_2*NHBoc), 40.00 (*CH_2*NHBoc, *CH_2*NH), 77.73 (Cq tBu), 114.96 (CH 1), 115.78 (CH 6), 122.88 (CH 7), 124.66 (Cq 5a), 126.59 (CH 9), 126.74 (CH 8), 132.15 (CH 2), 132.93 (Cq 3a), 137.42 (Cq 9a), 147.74 (Cq 4), 156.04 (C=O carbamate). MS (ESI +, QTof, m/z): 384.24 $[M+H]^+$

*tert-butyl 4-(imidazo[1,2-a]quinoxalin-4-yl)piperazine-1-carboxylate (**6h**).* Yield: 63%. $C_{19}H_{23}N_5O_2$. Mw: 353.42 g/mol. Mp: 154°C. ^{1}H-NMR δ (ppm, 400 MHz, DMSO d_6) 1.44 (s, 9H, 3 x CH_3 tBu), 3.51 (m, 4H, 2 x *CH_2*NBoc), 4.30 (m, 4H, 2 x *CH_2*NC=N), 7.33 (t, 1H, CH 7, *J=8Hz*), 7.44 (t, 1H, CH 8, *J=8Hz*), 7.60 (d, 1H, CH 9, *J=8Hz*), 7.69 (d, 1H, CH 2, *J=4Hz*), 8.14 (d, 1H, CH 6, *J=8Hz*), 8.68 (d, 1H, CH 1, *J=4Hz*). ^{13}C-NMR δ (ppm, 100 MHz, DMSO d_6) 28.54 (CH_3 tBu), 44.5 (*CH_2*NBoc), 46.06 (*CH_2*NC=N), 79.52 (Cq tBu), 114.82 (CH 1), 115.67 (CH 6), 124.01 (CH 7), 124.98 (Cq 5a), 126.97 (CH 9, CH 8), 136.03 (CH 2), 132.52 (Cq 3a), 136.03 (Cq 9a), 147.53 (Cq 4), 154.44 (C=O carbamate). MS (ESI +, QTof, m/z): 354.19 $[M+H]^+$

4.1.7. Procedure for the introduction of the methoxy group.

Sodium methanolate (0.59 mmol) was added to **5** (0.1 mmol) in methanol (5 mL) in a microwave-adapted vial and sealed. The reaction was submitted to microwave irradiations at 70°C for 2 min and

then evaporated. The residue was dissolved in dichloromethane and washed with brine. The organic layer was dried over $MgSO_4$, filtered and concentrated under reduced pressure to afford **6j**.

*4-methoxyimidazo[1,2-a]quinoxaline (**6j**).* Yield: 89%. $C_{11}H_9N_3O$. Mw: 199.21 g/mol. Mp: 169°C. ^{1}H-NMR δ (ppm, 400 MHz, DMSO d_6) 4.14 (s, 3H, O*CH*$_3$), 7.56 (m, 2H, CH 7, CH 8), 7.73 (s, 1H, CH 2), 7.81 (s, 1H, CH 9), 8.29 (s, 1H, CH 6), 8.76 (s, 1H, CH 1). ^{13}C-NMR δ (ppm, 100 MHz, DMSO d_6) 54.19 (O*CH*$_3$), 115.78 (CH 1), 116.22 (CH 6), 126.37 (Cq 5a), 126.50 (CH 8), 127.15 (CH 7), 128.01 (CH 9), 132.36 (Cq 3a), 133.59 (CH 2), 134.40 (Cq 9a), 153.25 (Cq 4). MS (ESI +, QTof, m/z): 200.2 $[M+H]^+$

4.1.8. Procedure for the introduction of the amino group.

A 30% (w/v) ammoniac aqueous solution (78.6 mmol) was added to a solution of **5** (9.8 mmol) in acetonitrile (10 mL) in a microwave-adapted vial. The reaction was submitted to microwave irradiations during 2 hours at 140°C. The solvent was removed under reduced pressure. The crude mixture was purified by flash chromatography eluted with cyclohexane/ethyl acetate to afford compound **6k** as a white solid.

*Imidazo[1,2-a]quinoxalin-4-amine (**6k**).* Yield: 84%. $C_{10}H_8N_4$. Mw: 184.19 g/mol. Mp: 183°C. ^{1}H-NMR δ (ppm, 400 MHz, DMSO d_6) 7.24 (s, 2H, NH_2),), 7.32 (t, 1H, CH 7, *J=8Hz*), 7.40 (t, 1H, CH 8, *J=8Hz*), 7.54 (d, 1H, CH 9, *J=8Hz*), 7.64 (s, 1H, CH 2, *J=4Hz*), 8.09 (d, 1H, CH 6, *J=8Hz*), 8.61 (s, 1H, CH 1, *J=4Hz*). ^{13}C-NMR δ (ppm, 100 MHz, DMSO d_6) 115.15 (CH 1), 115.88 (CH 6), 123.14 (CH 7), 124.99 (Cq 5a), 126.04 (CH 9), 126.78 (CH 8), 132.48 (CH 2), 132.72 (Cq 3a), 137.21 (Cq 9a), 149.26 (Cq 4). MS (ESI +, QTof, m/z): 185.10 $[M+H]^+$

4.1.9. General procedure for bromination.

A solution of **6** (3.5 mmol) and *N*-bromosuccinimide (3.85 mmol) in chloroform (100 mL) was heated under reflux for 2 hours. The solvent was evaporated under vacuum and the residue was dissolved in ethyl acetate, washed twice with a saturated aqueous NH_4Cl solution, saturated aqueous $NaHCO_3$ solution, distillated water, brine, then dried over Na_2SO_4, filtered and concentrated under vacuum. Compounds **7** are used without further purification as the reaction is considered as complete.

*1-bromo-N-methyl-7-(trifluoromethyl)imidazo[1,2-a]quinoxalin-4-amine (**7a**).* $C_{12}H_8BrF_3N_4$. Mw: 345.12 g/mol. Mp: 187°C. ^{1}H-NMR δ (ppm, 400 MHz, DMSO d_6) 3.04 (d, 3H, *CH*$_3$NH, *J=8Hz*), 7.65 (m, 2H, CH 8), 7.78 (s, 1H, CH 2), 7.88 (s, 1H, CH 6), 8.11 (m, 1H, *NH*CH_3), 9.12 (d, 1H, CH 9, *J=8Hz*). ^{19}F-RMN δ (ppm, 376.5 MHz, DMSO d6) -60.42. ^{13}C-NMR δ (ppm, 100 MHz, DMSO d_6) 27.71 (*CH*$_3$NH), 100.03 (Cq 1), 117.19 (CH 9), 118.43 (CH 8), 123.62 (CF_3), 127.74 (Cq 5a), 128.30 (CH 6), 132.72 (Cq 7), 134.29 (Cq 3a), 135.00 (CH 2), 138.56 (Cq 9a), 148.68 (Cq 4). MS (ESI +, QTof, m/z): 344.90 $[M+H]^+$

*1-bromo-N-methyl-7-(trifluoromethoxy)imidazo[1,2-a]quinoxalin-4-amine (**7b**).* $C_{12}H_8BrF_3N_4O$. Mw: 361.12 g/mol. Mp: 181°C. ^{1}H-NMR δ (ppm, 400 MHz, DMSO d_6) 3.02 (d, 3H, *CH*$_3$NH, *J=8Hz*), 7.30 (d, 1H, CH 8, *J=8Hz*), 7.51 (s, 1H, CH 6), 7.73 (s, 1H, CH 2), 8.05 (m, 1H, *NH*CH_3), 9.02 (d, 1H, CH 9, *J=8Hz*). ^{13}C-NMR δ (ppm, 100 MHz, DMSO d_6) 27.70 (*CH*$_3$NH), 99.85 (Cq 1), 114.79 (CH 8), 116.88 (CH 9), 119.34 (CH 6), 121.89 (CF_3), 124.80 (Cq 5a), 134.19 (CH 2), 134.71 (Cq 3a), 139.55 (Cq 9a), 146.82 (Cq 7), 148.03 (Cq 4). ^{19}F-RMN δ (ppm, 376.5 MHz, DMSO d6) -56.77. MS (ESI +, QTof, m/z): 360.90 $[M+H]^+$

*1-bromo-N-methyl-8-(trifluoromethyl)imidazo[1,2-a]quinoxalin-4-amine (**7c**).* $C_{12}H_8BrF_3N_4$. Mw: 345.12 g/mol. Mp: 194°C. ^{1}H-NMR δ (ppm, 400 MHz, DMSO d_6) 3.04 (d, 3H, *CH*$_3$NH, *J=8Hz*), 7.75 (m,

3H, CH 2, CH 6, CH 7), 8.21 (m, 1H, NH), 9.24 (s, 1H, CH 9). ^{13}C-NMR δ (ppm, 100 MHz, DMSO d_6) 27.73 (*CH*$_3$NH), 100.32 (Cq 1), 112.26 (CH 9), 123.60 and 123.63 (CF_3, CH 7), 125.58 (Cq 5a), 126.18 (Cq 8), 127.81 (CH 6), 134.25 (Cq 3a), 134.83 (CH 2), 141.44 (Cq 9a), 149.02 (Cq 4). ^{19}F-RMN δ (ppm, 376.5 MHz, DMSO d6) -59.89 (CF_3). MS (ESI +, QTof, m/z): 344.90 $[M+H]^+$

*tert-butyl (2-((1-bromoimidazo[1,2-a]quinoxalin-4-yl)amino)ethyl)carbamate (**7e**).* $C_{17}H_{20}BrN_5O_2$. Mw: 406.28 g/mol. Mp: 137°C. ^{1}H-NMR δ (ppm, 400 MHz, DMSO d_6) 1.36 (s, 9H, 3 x CH_3 tBu), 3.26 (m, 2H, *CH*$_2$NHBoc), 3.59 (m, 2H, *CH*$_2$NH), 6.98 (m, 1H, *NH*Boc), 7.30 (t, 1H, CH 7, *J=8Hz*), 7.35 (t, 1H, CH 8, *J=8Hz*), 7.61 (d, 1H, CH 9, *J=8Hz*), 7.72 (m, 2H, CH 2, NH), 8.96 (d, 1H, CH 6, *J=8Hz*). ^{13}C-NMR δ (ppm, 100 MHz, DMSO d_6) 28.68 (CH_3 tBu), 40.00 (*CH*$_2$NHBoc, *CH*$_2$NH), 78.09 (Cq tBu), 99.35 (Cq 1), 114.98 (CH 6), 122.66 (CH 7), 125.91 (Cq 5a), 127.34 (CH 8, CH 9), 134.20 (CH 2), 134.35 (Cq 3a), 138.03 (Cq 9a), 147.35 (Cq 4), 156.24 (C=O carbamate). MS (ESI +, QTof, m/z): 406.08 $[M+H]^+$.

*tert-butyl (3-((1-bromoimidazo[1,2-a]quinoxalin-4-yl)amino)propyl)carbamate (**7f**).* $C_{18}H_{22}BrN_5O_2$. Mw: 420.30 g/mol. Mp: 148°C. ^{1}H-NMR δ (ppm, 400 MHz, DMSO d_6) 1.38 (s, 9H, 3 x CH_3 tBu), 1.74 (m, 2H, *CH*$_2$CH$_2$NHBoc), 3.00 (qd, 2H, *CH*$_2$NHBoc, *J=4Hz*), 3.56 (qd, 2H, *CH*$_2$NH, *J=4Hz*), 6.90 (m, 1H, *NH*Boc), 7.54 (m, 3H, CH 7, CH 8, CH 9), 7.73 (s, 1H, CH 2, *J=4Hz*), 7.97 (m, 1H, NH), 9.04 (d, 1H, CH 6, *J=8Hz*). ^{13}C-NMR δ (ppm, 100 MHz, DMSO d_6) 28.71 (CH_3 tBu), 29.59 (*CH*$_2$CH$_2$NHBoc), 37.93 (*CH*$_2$NH, *CH*$_2$NHBoc), 77.95 (Cq tBu), 100.04 (Cq 1), 117.42 (CH 6), 126.66 (CH 7), 127.42 (Cq 5a), 128.59 (CH 8), 130.02 (CH 9), 134.03 (Cq 3a), 134.73 (CH 2), 137.24 (Cq 9a), 147.45 (Cq 4), 156.11 (C=O carbamate). MS (ESI +, QTof, m/z): 420.10 $[M+H]^+$

*tert-butyl (6-((1-bromoimidazo[1,2-a]quinoxalin-4-yl)amino)hexyl)carbamate (**7g**).* $C_{21}H_{28}BrN_5O_2$. Mw: 462.38 g/mol. Mp: 113°C. ^{1}H-NMR δ (ppm, 400 MHz, DMSO d_6) 1.29 to 1.40 (m, 15H, 3 x CH_3 tBu, *CH*$_2$CH$_2$CH$_2$NH, *CH*$_2$CH$_2$CH$_2$NHBoc, *CH*$_2$CH$_2$NHBoc), 1.63 (m, 2H, *CH*$_2$CH$_2$NH), 2.87 (qd, 2H, *CH*$_2$NHBoc, *J=4Hz*), 3.51 (qd, 2H, *CH*$_2$NH, *J=4Hz*), 6.76 (t, 1H, *NH*Boc, *J=4Hz*), 7.28 (t, 1H, CH 7, *J=8Hz*), 7.42 (t, 1H, CH 8, *J=8Hz*), 7.58 (d, 1H, CH 9, *J=8Hz*), 7.63 (s, 1H, CH 2), 7.74 (m, 1H, NH), 8.94 (d, 1H, CH 6, *J=8Hz*). ^{13}C-NMR δ (ppm, 100 MHz, DMSO d_6) 26.53 and 26.69 (*CH*$_2$CH$_2$CH$_2$NH, *CH*$_2$CH$_2$CH$_2$NHBoc), 28.73 (CH_3 tBu), 29.14 (*CH*$_2$CH$_2$NH), 29.93 (*CH*$_2$CH$_2$NHBoc), 40.00 (*CH*$_2$NHBoc, *CH*$_2$NH), 77.73 (Cq tBu), 99.39 (Cq 1), 114.96 (CH 6), 122.45 (CH 7), 125.73 (Cq 5a), 127.31 (CH 8, CH 9), 134.20 (Cq 3a), 134.50 (CH 2), 134.64 (Cq 9a), 149.14 (Cq 4), 156.03 (C=O carbamate). MS (ESI +, QTof, m/z): 462.15 $[M+H]^+$

*tert-butyl 4-(1-bromoimidazo[1,2-a]quinoxalin-4-yl)piperazine-1-carboxylate (**7h**).* $C_{19}H_{22}BrN_5O_2$. Mw: 432.31 g/mol. Mp: 139°C. ^{1}H-NMR δ (ppm, 400 MHz, DMSO d_6) 1.38 (s, 9H, 3 x CH_3 tBu), 3.45 (m, 4H, 2 x *CH*$_2$NBoc), 4.15 (m, 4H, 2 x *CH*$_2$NC=N), 7.28 (t, 1H, CH 7, *J=8Hz*), 7.44 (t, 1H, CH 8, *J=8Hz*), 7.54 (d, 1H, CH 9, *J=8Hz*), 7.70 (d, 1H, CH 2, *J=4Hz*), 8.93 (d, 1H, CH 6, *J=8Hz*). ^{13}C-NMR δ (ppm, 100 MHz, DMSO d_6) 28.53 (CH_3 tBu), 42.5 (*CH*$_2$NBoc), 46.42 (*CH*$_2$NC=N), 79.54 (Cq tBu), 99.64 (Cq 1), 114.97 (CH 6), 123.49 (CH 7), 126.11 (Cq 5a), 127.47 (CH 9, CH 8), 134.29 (CH 2), 134.66 (Cq 3a), 136.85 (Cq 9a), 147.33 (Cq 4), 154.43 (C=O carbamate). MS (ESI +, QTof, m/z): 432.10 $[M+H]^+$

*1-bromo-N,N-dimethylimidazo[1,2-a]quinoxalin-4-amine (**7i**).* $C_{12}H_{11}BrN_4$. Mw: 291.14 g/mol. Mp: 129°C. ^{1}H-NMR δ (ppm, 400 MHz, DMSO d_6) 3.50 (s, 6H, 2 x CH_3), 7.27 (td, 1H, CH 7, *J=8Hz, J=1.4Hz*), 7.43 (td, 1H, CH 8, *J=8Hz, J=1.4Hz*), 7.58 (dd, 1H, CH 9, *J=8Hz, J=1.4Hz*), 7.71 (s, 1H, CH 2), 8.96 (dd, 1H, CH 6, *J=8Hz, J=1.4Hz*). ^{13}C-NMR δ (ppm, 100 MHz, DMSO d_6) 40.00 (2 x CH_3), 99.43 (Cq 1), 114.88 (CH 6), 122.41 (CH 7), 125.77 (Cq 5a), 127.06 (CH 9), 127.30 (CH 8), 134.38 (CH 2), 134.90 (Cq 3a), 135.51 (Cq 9a), 147.98 (Cq 4). MS (ESI +, QTof, m/z): 290.9 $[M+H]^{+\cdot}$

*1-bromo-4-methoxyimidazo[1,2-a]quinoxaline (**7j**).* $C_{11}H_8BrN_3O$. Mw: 278.10 g/mol. Mp: 148°C. ^{1}H-NMR δ (ppm, 400 MHz, DMSO d_6) 4.19 (s, 3H, OCH_3), 7.67 (m, 2H, CH 7, CH 8), 7.74 (s, 1H, CH 2), 7.92 (m, 1H, CH 9), 9.16 (m, 1H, CH 6). ^{13}C-NMR δ (ppm, 100 MHz, DMSO d_6) 54.33 (OCH_3), 100.29 (Cq 1), 115.29 (CH 6), 125.95 (CH 7, Cq 5a), 127.66 (CH 8), 128.60 (CH 9), 133.86 (Cq 3a), 135.25 (Cq 9a), 135.89 (CH 2), 152.74 (Cq 4). MS (ESI +, QTof, m/z): 277.8 $[M+H]^{+\cdot}$

*1-bromoimidazo[1,2-a]quinoxalin-4-amine (**7k**).* $C_{10}H_7BrN_4$. Mw: 263.09 g/mol. Mp: 134°C. ^{1}H-NMR δ (ppm, 400 MHz, DMSO d_6) 7.24 (s, 2H, NH_2), 7.30 (td, 1H, CH 7, *J=8Hz, J=1.4Hz*), 7.40 (td, 1H, CH 8, *J=8Hz, J=1.4Hz*), 7.59 (dd, 1H, CH 9, *J=8Hz, J=1.4Hz*), 7.72 (s, 1H, CH 2), 8.97 (dd, 1H, CH 6, *J=8Hz, J=1.4Hz*). ^{13}C-NMR δ (ppm, 100 MHz, DMSO d_6) 99.41 (Cq 1), 115.00 (CH 6), 122.54 (CH 7), 126.20 (Cq 5a), 126.79 (CH 9), 127.29 (CH 8), 134.06 (Cq 3a), 134.72 (CH 2), 138.25 (Cq 9a), 148.93 (Cq 4). MS (ESI +, QTof, m/z): 263.00 $[M+H]^{+\cdot}$

4.1.11. General procedure for the Suzuki-Miyaura cross-coupling.

To a mixture of **7** (1.53 mmol) in DME/H_2O (v/v, 1/1, 10 mL) were added 3,4-dimethoxyphenylboronic acid (1.84 mmol), tetrakis(triphenylphosphine) palladium (0.077 mmol) and sodium carbonate (3.06 mmol) in a microwave-adapted vial and sealed. The reaction was submitted to microwave irradiations during 20 minutes at 150°C and then filtered on a Celite pad. The filtrate was concentrated under reduced pressure and purified by flash chromatography eluted with cyclohexane/ethyl acetate to ethyl acetate/methanol to afford **8** as solid.

*EAPB02203-7a: 1-(3,4-dimethoxyphenyl)-N-methyl-7-(trifluoromethyl)imidazo[1,2-a]quinoxalin-4-amine (**8a**).* Yield: 13%. $C_{20}H_{17}F_3N_4O_2$. Mw: 402.37 g/mol. Mp: 165°C. ^{1}H-NMR δ (ppm, 400 MHz, DMSO d_6) 3.06 (d, 3H, CH_3NH, *J=8Hz*), 3.75 (s, 3H, OCH_3), 3.87 (s, 3H, OCH_3), 7.15 (m, 2H, CH 5', CH 6'), 7.20 (s, 1H, CH 2'), 7.33 (d, 1H, CH 8, *J=8Hz*), 7.45 (d, 1H, CH 9, *J=8Hz*), 7.54 (s, 1H, CH 2), 7.85 (s, 1H, CH 6), 8.05 (m, 1H, *NH*CH_3). ^{13}C-NMR δ (ppm, 100 MHz, DMSO d_6) 27.72 (CH_3NH), 56.03 (OCH_3), 56.16 (OCH_3), 112.37 (CH 5'), 114.01 (CH 2'), 117.09 (CH 9), 118.97 (CH 8), 122.18 (Cq 1'), 122.88 (CH 6, CH 6'), 125.85 (CF_3), 126.34 (Cq 5a), 131.29 (Cq 1), 132.82 (CH 2), 133.01 (Cq 3a), 137.53 (Cq 9a), 138.47 (Cq 7), 149.27 (Cq 3', Cq 4'), 150.22 (Cq 4). ^{19}F-RMN δ (ppm, 400 MHz, DMSO d_6) -60.42. MS (ESI +, QTof, m/z): 403.00 $[M+H]^+$

*EAPB02203-7b: 1-(3,4-dimethoxyphenyl)-N-methyl-7-(trifluoromethoxy)imidazo[1,2-a]quinoxalin-4-amine (**8b**).* Yield: 67%. $C_{20}H_{17}F_3N_4O_3$. Mw: 418.37 g/mol. Mp: 169°C. ^{1}H-NMR δ (ppm, 400 MHz, DMSO d_6) 3.08 (d, 3H, CH_3NH, *J=8Hz*), 3.77 (s, 3H, OCH_3), 3.88 (s, 3H, OCH_3), 7.01 (d, 1H, CH 8, *J=8Hz*), 7.12 (d, 1H, CH 6', *J=8Hz*), 7.17 (d, 1H, CH 5', *J=8Hz*), 7.20 (s, 1H, CH 2'), 7.36 (d, 1H, CH 9), 7.48 (s, 1H, CH 6), 7.51 (d, 1H, CH 2, *J=4Hz*), 8.02 (d, 1H, *NH*CH_3, *J=4Hz*). ^{13}C-NMR δ (ppm, 100 MHz, DMSO d_6) 27.75 (CH_3NH), 56.01 (OCH_3), 56.14 (OCH_3), 112.34 (CH 5'), 114.14 (CH 2'), 114.59 (CH 8), 117.23 (CH 9), 118.12 (CH 6), 122.35 (Cq 1'), 123.29 (CH 6'), 124.01 (Cq 5a), 124.40 (CF_3), 131.01 (Cq 1), 132.56 (CH 2), 133.24 (Cq 3a), 139.82 (Cq 9a), 146.29 (Cq 7), 149.27 and 149.36 (Cq 4', Cq 3'), 150.20 (Cq 4). ^{19}F-RMN δ (ppm, 376.5 MHz, DMSO d6) -56.86 (OCF_3). MS (ESI +, QTof, m/z): 419.20 $[M+H]^+$. HRMS calculated for $C_{20}H_{18}F_3N_4O_3$ 419.1326, found 419.1329.

*EAPB02203-8a: 1-(3,4-dimethoxyphenyl)-N-methyl-8-(trifluoromethyl)imidazo[1,2-a]quinoxalin-4-amine (**8c**).* Yield: 21%. $C_{20}H_{17}F_3N_4O_2$. Mw: 402.37 g/mol. Mp: 179°C. ^{1}H-NMR δ (ppm, 400 MHz, DMSO d_6) 2.94 (d, 3H, CH_3NH), 3.75 (s, 3H, OCH_3), 3.86 (s, 3H, OCH_3), 7.16 (m, 2H, CH 5', CH 6'), 7.23 (s, 1H, CH 2'), 7.55 (s, 1H, CH 2), 7.59 (m, 2H, CH 7, CH 9), 7.72 (d, 1H, CH 6, *J=8Hz*), 8.16 (m, 1H, NH).

^{13}C-NMR δ (ppm, 100 MHz, DMSO d_6) 29.42 (CH_3NH), 56.18 (OCH_3), 56.24 (OCH_3), 112.55 (CH 5'), 113.31 (CH 9), 114.22 (CH 2'), 122.12 (Cq 1'), 122.765 (CH 7), 123.46 (CH 6'), 125.40 (Cq 5a),127.53 (CH 6), 129.18 (CF_3), 131.21 (Cq 1), 132.53 (CH 2), 133.36 (Cq 3a), 141.46 (Cq 9a), 142.19 (Cq 8), 149.55 (Cq 3', Cq 4'), 150.47 (Cq 4). ^{19}F-RMN δ (ppm, 376.5 MHz, DMSO d6) -60.28. MS (ESI +, QTof, m/z): 403.00 $[M+H]^+$. HRMS calculated for $C_{20}H_{18}F_3N_4O_2$ 403.1376, found 403.1385.

*EAPB02203: 1-(3,4-dimethoxyphenyl)-N-methylimidazo[1,2-a]quinoxalin-4-amine (**8d**).* Yield: 47%. $C_{19}H_{18}N_4O_2$. Mw: 334.37 g/mol. Mp: 168°C. ^{1}H-NMR δ (ppm, 400 MHz, DMSO d_6) 3.09 (s, 3H, $NHCH_3$), 3.69 (s, 3H, OCH_3), 3.79 (s, 3H, OCH_3), 7.03 (t, 1H, CH 7, *J=8Hz*), 7.13 (m, 3H, CH 2', CH 5', CH 6'), 7.26 (d, 1H, CH 6, *J=8Hz*), 7.36 (t, 1H, CH 8, *J=8Hz*), 7.51 (s, 1H, CH 2), 7.69 (d, 1H, CH 9, *J=8Hz*). ^{13}C-NMR δ (ppm, 100 MHz, DMSO d_6) 27.26 ($NHCH_3$), 54.87 (OCH_3), 54.93 (OCH_3), 111.10 (CH 6'), 112.47 (CH 2'), 115.03 (CH 6), 120.87 (Cq 1'), 122.32 and 122.40 (CH 7, CH 5'), 123.57 (Cq 5a), 123.92 (CH 8), 126.26 (CH 9), 130.70 (Cq 1), 131.68 and 131.89 (CH 2, Cq 3a), 133.58 (Cq 9a), 146.62 (Cq 3'), 147.90 (Cq 4'), 148.93 (Cq 4). MS (ESI +, QTof, m/z): 335.20 $[M+H]^+$. HRMS calculated for $C_{19}H_{19}N_4O_2$ 335.1518, found 335.1503.

*EAPB02211: tert-butyl (2-((1-(3,4-dimethoxyphenyl)imidazo[1,2-a]quinoxalin-4-yl)amino)ethyl)carbamate (**8e**).* Yield: 57%. $C_{25}H_{29}N_5O_4$. Mw: 463.53 g/mol. Mp: 168°C. ^{1}H-NMR δ (ppm, 400 MHz, DMSO d_6) 1.38 (s, 9H, 3 x CH_3 tBu), 3.27 (qd, 2H, CH_2NHBoc, *J=8Hz*), 3.63 (qd, 2H, CH_2NH, *J=8Hz*), 3.74 (s, 3H, OCH_3), 3.87 (s, 3H, OCH_3), 6.98 (m, 2H, *NH*Boc, CH 7), 7.16 (m, 3H, CH 2', CH 5', CH 6'), 7.30 (m, 2H, CH 8, CH 6), 7.49 (s, 1H, CH 2), 7.58 (d, 2H, CH 9, *J=8Hz*), 7.71 (t, 1H, NH, *J=4Hz*). ^{13}C-NMR δ (ppm, 100 MHz, DMSO d_6) 28.70 (CH_3 tBu), 40.00 (CH_2NHBoc, CH_2NH), 56.05 (OCH_3), 56.15 (OCH_3), 78.10 (Cq tBu), 112.30 (CH 2'), 114.19 (CH 5'), 115.88 (CH 6), 122.35 (Cq 1'), 122.76 (CH 7), 123.26 (CH 6'), 125.84 (Cq 5a), 126.49 (CH 8), 127.09 (CH 9), 130.85 (Cq 1), 132.42 (CH 2), 133.30 (Cq 3a), 138.06 (Cq 9a), 148.00 (Cq 3'), 149.25 (Cq 4'), 150.10 (Cq 4), 156.25 (C=O carbamate). MS (ESI +, QTof, m/z): 464.23 $[M+H]^+$. HRMS calculated for $C_{25}H_{30}N_5O_4$ 464.2292, found 464.2294.

*EAPB02214 : tert-butyl (3-((1-(3,4-dimethoxyphenyl)imidazo[1,2-a]quinoxalin-4-yl)amino)propyl)carbamate (**8f**).* Yield: 69%. $C_{26}H_{31}N_5O_4$. Mw: 477.56 g/mol. Mp: 171°C. ^{1}H-NMR δ (ppm, 400 MHz, DMSO d_6) 1.36 (s, 9H, 3 x CH_3 tBu), 1.77 (m, 1H, CH_2CH_2NHBoc), 3.02 (qd, 2H, CH_2NHBoc, *J=4Hz*), 3.56 (qd, 2H, CH_2NH, *J=4Hz*), 3.74 (s, 3H, OCH_3), 3.89 (s, 3H, OCH_3), 6.97 (m, 2H, CH 7, NHBoc), 7.17 (m, 3H, CH 6', CH 2', CH 5'), 7.29 (m, 2H, CH 6, CH 8), 7.49 (s, 1H, CH 2), 7.61 (m, 1H, CH 9). ^{13}C-NMR δ (ppm, 100 MHz, DMSO d_6) 28.73 (CH_3 tBu), 29.80 (CH_2CH_2NHBoc), 37.91 (CH_2NHBoc, CH_2NH), 56.05 (OCH_3), 56.15 (OCH_3), 77.95 (Cq tBu), 112.30 (CH 5'), 114.22 (CH 2'), 115.92 (CH 6), 122.27 (Cq 1'), 123.28 (CH 7, CH 6'), 125.73 to 127.93 (CH 8, CH 9, Cq 5a), 130.85 (Cq 1), 132.43 (CH 2), 133.13 (Cq 3a), 139.56 (Cq 9a), 147.95 (Cq 3'), 149.25 (Cq 4'), 150.11 (Cq 4), 156.12 (C=O carbamate). MS (ESI +, QTof, m/z): 478.25 $[M+H]^+$. HRMS calculated for $C_{26}H_{32}N_5O_4$ 478.2454, found 478.2456.

*EAPB02212: tert-butyl (6-((1-(3,4-dimethoxyphenyl)imidazo[1,2-a]quinoxalin-4-yl)amino)hexyl)carbamate (**8g**).* Yield: 61%. $C_{29}H_{37}N_5O_4$. Mw: 519.64 g/mol. Mp: 133°C. ^{1}H-NMR δ (ppm, 400 MHz, DMSO d_6) 1.31 to 1.40 (m, 15H, 3 x CH_3 tBu, $CH_2CH_2CH_2$NH, $CH_2CH_2CH_2$NHBoc, CH_2CH_2NHBoc), 1.66 (qt, 2H, CH_2CH_2NH, *J=8Hz*), 2.91 (qd, 2H, CH_2NHBoc, *J=4Hz*), 3.53 (qd, 2H, CH_2NH, *J=4Hz*), 3.74 (s, 3H, OCH_3), 3.87 (s, 3H, OCH_3), 6.77 (t, 1H, *NH*Boc, *J=4Hz*), 6.95 (t, 1H, CH 7, *J=8Hz*), 7.10 (m, 3H, CH 2', CH 5', CH 6'), 7.28 (m, 2H, CH 6, CH 8), 7.47 (s, 1H, CH 2), 7.57 (d, 1H, CH 9, *J=8Hz*), 7.67 (t, 1H, NH, *J=4Hz*). ^{13}C-NMR δ (ppm, 100 MHz, DMSO d_6) 26.5 and 26.72 ($CH_2CH_2CH_2$NH,

CH$_2$CH$_2$CH$_2$NHBoc), 28.74 (CH$_3$ tBu), 29.30 (*CH*$_2$CH$_2$NH), 29.97 (*CH*$_2$CH$_2$NHBoc), 40.00 (*CH*$_2$NHBoc, *CH*$_2$NH), 56.04 (OCH$_3$), 56.14 (OCH$_3$) 77.74 (Cq tBu), 112.28 (CH 2'), 114.23 (CH 5'), 115.85 (CH 6), 122.05 (CH 7), 122.84 (Cq 1'), 123.27 (CH 6'), 125.73 (Cq 5a), 126.44 (CH 8), 127.05 (CH 9), 130.79 (Cq 1), 132.31 (CH 2), 133.35 (Cq 3a), 138.31 (Cq 9a), 147.96 (Cq 3'), 149.24 (Cq 4'), 150.08 (Cq 4), 156.05 (C=O carbamate). MS (ESI +, QTof, m/z): 520.29 [M+H]$^+$. HRMS calculated for $C_{29}H_{38}N_5O_4$ 520.2918, found 520.2925.

*EAPB02213: tert-butyl 4-(1-(3,4-dimethoxyphenyl)imidazo[1,2-a]quinoxalin-4-yl)piperazine-1-carboxylate (**8h**).* Yield: 85%. $C_{27}H_{31}N_5O_4$. Mw: 489.57 g/mol. Mp: 170°C. ^{1}H-NMR δ (ppm, 400 MHz, DMSO d$_6$) 1.45 (s, 9H, 3 x CH$_3$ tBu), 3.53 (m, 4H, 2 x *CH*$_2$NBoc), 3.73 (s, 3H, O*CH*$_3$), 3.87 (s, 3H, O*CH*$_3$), 4.29 (m, 4H, 2 x *CH*$_2$NC=N), 7.05 (t, 1H, CH 7, *J=8Hz*), 7.10 (d, 1H, CH 6'), 7.15 (m, 2H, CH 2', CH 5'), 7.30 (d, 1H, CH 6, *J=8Hz*), 7.35 (t, 1H, CH 8, *J=8Hz*), 7.56 (s, 1H, CH 2), 7.63 (d, 1H, CH 9, *J=8Hz*). ^{13}C-NMR δ (ppm, 100 MHz, DMSO d$_6$) 28.56 (CH3 tBu), 43.00 (*CH*$_2$NBoc), 46.40 (*CH*$_2$NC=N), 56.07 (OCH$_3$), 56.16 (OCH$_3$), 79.54 (Cq tBu), 112.36 (CH 5'), 114.12 (CH 2'), 115.81 (CH 6), 122.79 (CH 7), 123.23 (CH 6', Cq 1'), 125.73 (Cq 5a), 126.44 (CH 8), 127.35 (CH 9), 130.36 (Cq 1), 132.51 (CH 2), 133.35 (Cq 3a), 136.91 (Cq 9a), 147.94 (Cq 3'), 149.33 (Cq 4'), 150.18 (Cq 4), 154.46 (C=O carbamate). MS (ESI +, QTof, m/z): 490.25 [M+H]$^+$. HRMS calculated for $C_{27}H_{32}N_5O_4$ 490.2449, found 490.2451.

*EAPB02204: 1-(3,4-dimethoxyphenyl)-N,N-dimethylimidazo[1,2-a]quinoxalin-4-amine (**8i**).* Yield: 28%. $C_{20}H_{20}N_4O_2$. Mw: 348.40 g/mol. Mp: 185°C. ^{1}H-NMR δ (ppm, 400 MHz, DMSO d$_6$) 3.74 (s, 3H, CH$_3$), 3.78 (s, 3H, CH$_3$), 3.84 (s, 3H, CH$_3$), 3.87 (s, 3H, CH$_3$), 7.02 (m, 2H, CH 7, CH 6'), 7.15 (m, 3H, CH 2, CH 2', CH 5'), 7.26 (d, 1H, CH 6, *J = 8Hz*), 7.33 (t, 1H, CH 8, *J = 8Hz*), 7.64 (m, 1H, CH 9). ^{13}C-NMR δ (ppm, 100 MHz, DMSO d$_6$) 56.07 (4 x CH3), 110.89 (CH 5'), 112.37 (CH 2'), 112.63 (CH 6'), 115.94 (CH 6), 118.99 (CH 2), 122.21 (CQ 1', Cq 5'), 122.64 (CH 7), 125.44 (Cq 3'), 126.78 (CH 8), 132.73 (Cq 1), 132.73 (Cq 1), 133.59 (Cq 9'), 133.72 (CH 9), 148.54 (Cq 3'), 149.45 (Cq 4'), 150.23 (Cq 4). MS (ESI +, QTof, m/z): 349.20 [M+H]$^+$. HRMS calculated for $C_{20}H_{21}N_4O_2$ 349.1663, found 349.1665.

*EAPB02215: 1-(3,4-dimethoxyphenyl)-4-methoxyimidazo[1,2-a]quinoxaline (**8j**).* Yield: 32%. $C_{19}H_{17}N_3O_3$. Mw: 335.36 g/mol. Mp: 178°C. ^{1}H-NMR δ (ppm, 400 MHz, DMSO d$_6$) 3.75 (s, 3H, OCH$_3$), 3.88 (s, 3H, OCH$_3$), 4.16 (s, 3H, OCH$_3$), 7.18 (m, 3H, CH 2', CH 5', CH 6'), 7.28 (t, 1H, CH 8, *J=8Hz*), 7.42 (m, 2H, CH 7, CH 9), 7.56 (s, 1H, CH 2), 7.80 (d, 1H, CH 6, *J=8Hz*). ^{13}C-NMR δ (ppm, 100 MHz, DMSO d$_6$) 54.22 (OCH$_3$), 56.07 and 56.17 (2 x OCH$_3$), 112.34 (CH 5'), 114.16 (CH 2'), 116.10 (CH 9), 122.35 (Cq 1'), 123.29 (CH 6'), 125.61 (CH 8), 127.45 (CH 7), 127.98 (Cq 9a), 128.70 (CH 6), 131.32 (Cq 1), 132.76 (Cq 3a), 133.87 (CH 2), 135.24 (Cq 5), 149.32 (Cq 4'), 150.25 (Cq 3a), 153.41 (Cq 4). MS (ESI +, QTof, m/z): 335.9 [M+H]$^+$. HRMS calculated for $C_{19}H_{18}N_3O_3$ 336.1343, found 336.1348.

*EAPB02202: 1-(3,4-dimethoxyphenyl)-4-methoxyimidazo[1,2-a]quinoxaline (**8k**). Y*ield: 70%. $C_{18}H_{16}N_4O_2$. Mw: 320.34 g/mol. Mp: 178°C. ^{1}H-NMR δ (ppm, 400 MHz, DMSO d$_6$) 3.74 (s, 3H, OCH$_3$), 3.87 (s, 3H, OCH$_3$), 6.99 (t, 1H, CH 7, *J=8Hz*), 7.13 (m, 3H, CH 2', CH 5', CH 6'), 7.22 (m, 2H, CH 6, CH 8), 7.50 (s, 1H, CH 2), 7.56 (m, 2H, NH$_2$), 7.63 (d, 1H, CH 9, *J=8Hz*). ^{13}C-NMR δ (ppm, 100 MHz, DMSO d$_6$) 54.94 (OCH$_3$), 55.04 (OCH$_3$), 111.13 (CH 6'), 113.07 (CH 2'), 114.80 (CH 6), 121.15 (CH 7), 121.70 (Cq 1'), 122.19 (CH 5'), 125.01 (Cq 5a), 125.47 (CH 8), 128.11 (CH 9), 130.83 (Cq 1), 131.55 (CH 2), 132.04 (Cq 3a), 137.16 (Cq 9a), 148.12 (Cq 3'), 148.42 (Cq 4'), 148.96 (Cq 4). MS (ESI +, QTof, m/z): 321.10 [M+H]$^+$. HRMS calculated for $C_{18}H_{17}N_4O_2$ 336.1343, found 336.1348.

4.1.12. General procedure for the cleavage of all protections.

After solubilisation of compound **8** (0.411 mmol) in dichloromethane, boron tribromide (2 eq/protecting group) was slowly added at 0°C. The reaction was allowed to warm up to room temperature and stirred for 2 hours. Methanol was added to quench the reaction which was then concentrated under reduced pressure. The crude mixture was purified by flash chromatography eluted with ethyl acetate/methanol to afford **9** as solid.

*EAPB02303-7a: 4-(4-(methylamino)-7-(trifluoromethyl)imidazo[1,2-a]quinoxalin-1-yl)benzene-1,2-diol (**9a**).* Yield: 28%. $C_{18}H_{13}F_3N_4O_2$. Mw: 374.32 g/mol. Mp: 248°C. ^{1}H-NMR δ (ppm, 400 MHz, DMSO d_6) 3.06 (d, 3, CH_3NH, *J=8Hz*), 6.81 (d, 1H, CH 6', *J=8Hz*), 6.89 (s, 1H, CH 2'), 6.92 (d, 1H, CH 5', *J=8Hz*), 7.34 (d, 1H, CH 8, *J=8Hz*), 7.47 (s, 1H, CH 2), 7.51 (d, 1H, CH 9, *J=8Hz*), 7.82 (s, 1H, CH 6), 8.03 (m, 1H, *NH*CH_3). ^{19}F-RMN δ (ppm, 376.5 MHz, DMSO d6) -60.72 (CF_3). ^{13}C-NMR not available due to weak product amount. MS (ESI +, QTof, m/z): 375.10 $[M+H]^+$. HRMS calculated for $C_{18}H_{14}F_3N_4O_2$ 375.1063, found 375.1072.

*EAPB02303-7b: 4-(4-(methylamino)-7-(trifluoromethoxy)imidazo[1,2-a]quinoxalin-1-yl)benzene-1,2-diol (**9b**).* Yield: 67%. $C_{18}H_{13}F_3N_4O_3$. Mw: 390.32 g/mol. Mp: 255°C. ^{1}H-NMR δ (ppm, 400 MHz, DMSO d_6) 3.08 (d, 3H, *CH*$_3$NH, *J=8Hz*), 6.84 (d, 1H, CH 6', *J=8Hz*), 6.94 (s, 1H, CH 2'), 6.97 (d, 1H, CH 5', *J=8Hz*), 7.03 (d, 1H, CH 8, *J=8Hz*), 7.40 (d, 1H, CH 9, *J=8Hz*), 7.42 (s, 1H, CH 2), 7.45 (s, 1H, CH 6), 8.01 (d, 1H, *NH*CH_3, *J=4Hz*). ^{13}C-NMR δ (ppm, 100 MHz, DMSO d_6) 27.74 (*CH*$_3$NH), 114.58 (CH8), 116.56 (CH 5'), 117.15 (CH 9), 117.72 (CH 2'), 118.12 (CH 6), 120.80 (Cq 1'), 121.99 (CH 6'), 124.76 (Cq 5a), 131.38 (Cq 1), 132.20 (CH 2), 133.04 (Cq 3a), 139.79 (Cq 9a), 146.12 (Cq 3'), 146.25 (Cq 7), 147.18 (Cq 4'), 149.27 (Cq 4). ^{19}F-RMN δ (ppm, 376.5 MHz, DMSO d6) -56.83 (OCF_3). MS (ESI +, QTof, m/z): 391.10 $[M+H]^+$. HRMS calculated for $C_{18}H_{14}F_3N_4O_3$ 391.1013, found 391.1018.

*EAPB02303-8a: 4-(4-(methylamino)-8-(trifluoromethyl)imidazo[1,2-a]quinoxalin-1-yl)benzene-1,2-diol (**9c**).* Yield: 19%. $C_{18}H_{13}F_3N_4O_2$. Mw: 374.32 g/mol. Mp: 259°C. ^{1}H-NMR δ (ppm, 400 MHz, DMSO d_6) 3.12 (d, 3H, *CH*$_3$NH, *J=8Hz*), 6.83 (d, 1H, CH 6', *J=8Hz*), 6.91 (s, 1H, CH 2'), 6.96 (d, 1H, CH 5'), 7.55 (s, 1H, CH 2), 7.60 (s, 1H, CH 9), 7.67 (d, 1H, CH 7, *J=8Hz*), 7.82 (d, 1H, CH 6). ^{13}C-NMR δ (ppm, 100 MHz, DMSO d_6) 28.38 (*CH*$_3$NH), 113.45 (CH 9), 116.52 (CH 5'), 118.50 (CH 2'), 120.08 (Cq 1'), 121.93 (CH 1'), 123.11 (CH 7), 125.08 (Cq 5a), 132.68 to 132.75 (CH 2, Cq 1, Cq 3a, Cq 9a), 146.36 (Cq 3', Cq 4'), 147.49 (Cq 4). ^{19}F-RMN δ (ppm, 376.5 MHz, DMSO d6) -60.44 (CF_3). MS (ESI +, QTof, m/z): 375.20 $[M+H]^+$. HRMS calculated for $C_{18}H_{14}F_3N_4O_2$ 375.1063, found 375.1070.

*EAPB02303: 4-(4-(methylamino)imidazo[1,2-a]quinoxalin-1-yl)benzene-1,2-diol (**9d**).* Yield: 96 %. $C_{17}H_{14}N_4O_2$. Mw: 306.31 g/mol. Mp: 267°C. ^{1}H-NMR δ (ppm, 400 MHz, DMSO d_6) 3.04 (d, 3H, NH*CH3*, *J=4Hz*), 6.80 (dd, 1H, CH 6', *J=4Hz, J=8Hz*), 6.88 (d, 1H, CH 2', *J=4Hz*), 6.89 (d, 1H, CH 5', *J=8Hz*), 6.97 (td, 1H, CH 7, *J=8Hz, J=4Hz*), 7.31 (m, 2H, CH 6, CH 8), 7.39 (s, 1H, CH 2), 7.58 (dd, 1H, CH 9, *J=4Hz, J=8Hz*), 7.69 (qd, 1H, NH, *J=4Hz*). ^{13}C-NMR δ (ppm, 100 MHz, DMSO d_6) 27.25 (NHCH3), 115.86 (CH 6), 116.45 (CH 5'), 117.87 (CH 2'), 121.27 (Cq 1'), 122.00 (CH 6'), 122.08 (CH 7), 125.78 (Cq 5'), 126.38 (CH 8), 126.99 (CH 9), 131.12 (Cq 1), 131.98 (CH 2), 133.27 (Cq 3' quinoxaline), 138.28 (Cq 9'), 146.04 (Cq 3' phenyl), 147.07 (Cq 4' phenyl), 148.55 (Cq 4). MS (ESI +, QTof, m/z) : 307.12 $[M+H]^+$. HRMS calculated for $C_{17}H_{15}N_4O_2$ 307.1195, found 307.1194.

*EAPB02306: 4-(4-((2-aminoethyl)amino)imidazo[1,2-a]quinoxalin-1-yl)benzene-1,2-diol (**9e**).* Yield: 94%. $C_{18}H_{17}N_5O_2$. Mw: 335.36 g/mol. Mp: 263°C. ^{1}H-NMR δ (ppm, 400 MHz, DMSO d_6) 3.14 (m, 2H, *CH*$_2$$NH_2$), 3.81 (m, 2H, *CH*$_2$NH), 6.79 (d, 1H, CH 6', *J=8Hz*), 6.90 (s, 1H, CH 2'), 6.94 (d, 1H, CH 5', *J=8Hz*), 7.01 (t, 1H, CH 7, *J=8Hz*), 7.31 (m, 2H, CH 8, CH 6), 7.43 (s, 1H, CH 2), 7.60 (d, 1H, CH 9, *J=8Hz*),

7.87 (t, 1H, NH, *J=4Hz*). ^{13}C-NMR δ (ppm, 100 MHz, DMSO d_6) 40.00 (*CH*$_2$NH$_2$, *CH*$_2$NH), 115.83 (CH 6), 116.52 (CH 5'), 117.86 (CH 2'), 121.05 (Cq 1'), 121.96 (CH 6'), 122.71 (CH 7), 125.95 (Cq 5a), 126.52 (CH 8), 127.13 (CH 9), 131.34 (Cq 1), 132.13 (CH 2), 133.02 (Cq 3a), 137.65 (Cq 9a), 146.04 (Cq 3'), 147.10 (Cq 4'), 148.13 (Cq 4). MS (ESI +, QTof, m/z): 336.15 $[M+H]^+$. HRMS calculated for $C_{18}H_{18}N_5O_2$ 336.1455, found 336.1460.

*EAPB02309: 4-(4-((3-aminopropyl)amino)imidazo[1,2-a]quinoxalin-1-yl)benzene-1,2-diol (**9f**).* Yield: 80%. $C_{19}H_{19}N_5O_2$. Mw: 349.39 g/mol. Mp: 258°C. ^{1}H-NMR δ (ppm, 400 MHz, DMSO d_6) 2.00 (t, 2H, *CH*$_2$CH$_2$NH$_2$, *J=8Hz*), 2.90 (m, 2H, *CH*$_2$NH), 3.64 (m, 2H, *CH*$_2$NH$_2$), 6.80 (d, 1H, CH 6', *J=8Hz*), 6.94 (s, 1H, CH 2'), 6.96 (d, 1H, CH 5', *J=8Hz*), 7.01 (t, 1H, CH 7, *J=8Hz*), 7.30 (m, 2H, CH 6, CH 8), 7.46 (s, 1H, CH 2), 7.59 (d, 1H, CH 9, *J=8Hz*), 7.90 (m, 2H, NH$_2$). ^{13}C-NMR δ (ppm, 100 MHz, DMSO d_6) 27.54 (*CH*$_2$CH$_2$NH$_2$), 37.17 and 37.26 (*CH*$_2$NH$_2$, *CH*$_2$NH), 115.86 (CH 6), 116.48 (CH 5'), 117.88 (CH 2'), 121.14 (Cq 1'), 122.01 (CH 6'), 122.80 (CH 7), 124.80 (Cq 5a), 125.82 (CH 8), 126.46 (CH 9), 133.31 (Cq 1), 132.08 (CH 2), 133.01 (Cq 3a), 137.84 (Cq 9a), 146.00 (Cq 3'), 147.06 (Cq 4'), 148.08 (Cq 4). MS (ESI +, QTof, m/z): 350.16 $[M+H]^+$. HRMS calculated for $C_{19}H_{20}N_5O_2$ 350.1612, found 350.1615.

*EAPB02307: 4-(4-((6-aminohexyl)amino)imidazo[1,2-a]quinoxalin-1-yl)benzene-1,2-diol (**9g**).* Yield: 81%. $C_{22}H_{25}N_5O_2$. Mw: 391.47 g/mol. Mp: 251°C. ^{1}H-NMR δ (ppm, 400 MHz, DMSO d_6) 1.39 (m, 4H, *CH*$_2$CH$_2$CH$_2$NH, *CH*$_2$CH$_2$CH$_2$NH$_2$), 1.54 (m, 2H, *CH*$_2$CH$_2$NH$_2$), 1.69 (m, 2H, *CH*$_2$CH$_2$NH), 2.76 (m, 2H, *CH*$_2$NH$_2$), 3.57 (m, 2H, *CH*$_2$NH), 6.79 (d, 1H, CH 6', *J=8Hz*), 6.88 (s, 1H, CH 2'), 6.93 (d, 1H, CH 5', *J=8Hz*), 6.97 (t, 1H, CH 7), 7.29 (m, 2H, CH 6, CH8), 7.39 (s, 1H, CH 2), 7.54 (d, 1H, CH 9, *J=8Hz*), 7.64 (t, 1H, NH, *J=4Hz*). ^{13}C-NMR δ (ppm, 100 MHz, DMSO d_6) 26.08 and 26.53 (*CH*$_2$CH$_2$CH$_2$NH, *CH*$_2$CH$_2$CH$_2$NH$_2$), 27.47 (*CH*$_2$CH$_2$NH$_2$), 29.16 (*CH*$_2$CH$_2$NH), 40.00 (*CH*$_2$NH$_2$, *CH*$_2$NH), 115.85 (CH 6), 116.46 (CH 5'), 117.89 (CH 2'), 121.26 (Cq 1'), 122.09 (CH 7, CH 6'), 125.75 (Cq 5a), 126.41 (CH 8), 126.99 (CH 9), 131.22 (Cq 1), 131.96 (CH 2), 133.14 (Cq 3a), 138.24 (Cq 9a), 146.02 (Cq 3'), 147.05 (Cq 4'), 147.97 (Cq 4). MS (ESI +, QTof, m/z): 392.21 $[M+H]^+$. HRMS calculated for $C_{22}H_{26}N_5O_2$ 392.2081, found 392.2085.

*EAPB02308: 4-(4-(piperazin-1-yl)imidazo[1,2-a]quinoxalin-1-yl)benzene-1,2-diol (**9h**).* Yield: 54%. $C_{20}H_{19}N_5O_2$. Mw: 361.40 g/mol. Mp: 257°C. ^{1}H-NMR δ (ppm, 400 MHz, DMSO d_6) 3.09 (m, 4H, 2 x *CH*$_2$NH), 4.38 (m, 2H, 2 x *CH*$_2$NC=N), 6.79 (d, 1H, CH 6', *J=8Hz*), 6.88 (s, 1H, CH 2'), 6.92 (d, 1H, CH 5', *J=8Hz*), 7.04 (t, 1H, CH 7, *J=8Hz*), 7.34 (m, 3H, CH 6, CH 8, NH), 7.48 (s, 1H, CH 2), 7.60 (d, 1H, CH 9, *J=8Hz*), 7.95 (s, 1H, NH). ^{13}C-NMR not available due to weak product amount. MS (ESI +, QTof, m/z): 362.16 $[M+H]^+$. HRMS calculated for $C_{20}H_{20}N_5O_2$ 362.1612, found 362.1616.

*EAPB02304: 4-(4-(dimethylamino)imidazo[1,2-a]quinoxalin-1-yl)benzene-1,2-diol (**9i**).* Yield: 61%. $C_{18}H_{16}N_4O_2$. Mw: 320.34 g/mol. Mp: 247°C. ^{1}H-NMR δ (ppm, 400 MHz, DMSO d_6) 3.04 (2s, 6H, 2 x CH_3), 6.81 (dd, 1H, CH 6', *J=8Hz, J=1.5Hz*), 6.87 (d, 1H, CH 2', *J=1.5Hz*), 6.90 (d, 1H, CH 5', *J=8Hz*), 6.98 (td, 1H, CH 7, *J=8Hz, J=1.5Hz*), 7.27 (td, 1H, CH 8, *J=8Hz, J=1.5Hz*), 7.30 (d, 1H, CH 6, *J=8Hz*), 7.34 (s, 1H, CH 2), 7.60 (d, 1H, CH 9, *J=8Hz*). ^{13}C-NMR δ (ppm, 100 MHz, DMSO d_6) 115.38 (CH 6), 115.96 (CH 5'), 117.39 (CH 2'), 120.79 (Cq 1'), 121.52 (CH 6', CH 7), 125.30 (Cq 5a), 125.89 (CH 8), 126.50 (CH 9), 130.64 (Cq 1), 131.49 (CH 2), 132.79 (Cq 3a), 137.80 (Cq 9a), 145.55 (Cq 3'), 146.59 (Cq 4), 148.07 (Cq 4'). MS (ESI +, QTof, m/z): 321.03 $[M+H]^+$. HRMS calculated for $C_{18}H_{17}N_4O_2$ 321.1346, found 321.1352.

*EAPB02300: 4-(4-hydroxyimidazo[1,2-a]quinoxalin-1-yl)benzene-1,2-diol (**9j**).* Yield: 43%.$C_{16}H_{11}N_3O_3$. Mw: 293.28 g/mol. Mp: 261°C. ^{1}H-NMR δ (ppm, 400 MHz, DMSO d_6) 3.37 (m, 3H, OH), 6.79 (d, 1H, CH 6', *J=8Hz*), 6.87 (s, 1H, CH 2), 6.92 (d, 1H, CH 5), 7.00 (t, 1H, CH 8, *J=8Hz*), 7.23 (d, 1H, CH 9, *J=8Hz*), 7.31 (t, 1H, CH 7, *J=8Hz*), 7.37 (d, 1H, CH 6, *J=8Hz*), 7.40 (s, 1H, CH 2). ^{13}C-NMR δ (ppm, 100 MHz,

DMSO d_6) 116.53 (CH 5'), 116.73 (CH 9), 117.37 (CH 6), 117.64 (CH 2'), 120.74 (Cq 1'), 122.45 (CH 6'), 123.01 (CH 8), 124.30 (Cq 9a), 127.00 (CH 7), 129.63 (Cq 5), 132.35 (Cq 1), 133.22 (CH 2), 137.39 (Cq 3a), 146.12 (Cq 4'), 147.24 (Cq 3a), 153.21 (Cq 4). MS (ESI +, QTof, m/z): 294.1 $[M+H]^+$. HRMS calculated for $C_{16}H_{12}N_3O_3$ 294.0873, found 294.0877.

*EAPB 02302: 4-(4-aminoimidazo[1,2-a]quinoxalin-1-yl)benzene-1,2-diol (**9k**).* *Y*ield: 74%. $C_{16}H_{12}N_4O_2$.Mw: 292.29 g/mol. Mp: 264°C. ^{1}H-NMR δ (ppm, 400 MHz, DMSO d_6) 6.80 (dd, 1H, CH 6', J=4Hz, J=8Hz), 6.88 (d, 1H, CH 2', J=4Hz), 6.90 (d, 1H, CH 5', J=8Hz), 6.99 (td, 1H, CH 7, J=8Hz, J=4Hz), 7.13 (s, 2H, NH2), 7.32 (m, 2H, CH 6, CH 8), 7.42 (s, 1H, CH 2), 7.51 (dd, 1H, CH 9, J=4Hz, J=8Hz). ^{13}C-NMR δ (ppm, 100 MHz, DMSO d_6) 115.88 (CH 6), 116.46 (CH 5'), 117.87 (CH 2'), 121.24 (Cq 1'), 122.02 (CH 6'), 122.28 (CH 7), 126.08 (CH 9), 126.41 (CH 8, Cq 5'), 131.35 (Cq 1), 132.32 (CH 2), 132.92 (Cq 3' quinoxaline), 137.95 (Cq 9'), 146.02 (Cq 3' phenyl), 147.06 (Cq 4' phenyl), 149.48 (Cq 4). MS (ESI +, QTof, m/z) : 293.10 $[M+H]^+$. HRMS calculated for $C_{16}H_{13}N_4O_2$ 293.1039, found 293.1043.

4.1.13. General procedure for the preparation of ammonium chloride salts.

Compound **9** was solubilized in HCl/dioxane (4N) and stirred for 2 hours at room temperature. The reaction mixture was concentrated under reduced pressure, then dissolved in dichloromethane and concentrated again. The precipitate was crushed with diethyl ether and filtered to afford desired salt **10**.

*EAPB 02306s: 2-((1-(3,4-dihydroxyphenyl)imidazo[1,2-a]quinoxalin-4-yl)amino)ethanaminium chloride (**10e**).* $C_{18}H_{18}ClN_5O_2$. Mw: 371.82 g/mol. Mp: 221°C. ^{1}H-NMR δ (ppm, 400 MHz, DMSO d_6) 3.18 (m, 2H, *CH*$_2$NH$_3$), 4.05 (m, 2H, *CH*$_2$NH), 6.80 (d, 1H, CH 6', *J=8Hz*), 6.94 (s, 1H, CH 2'), 6.99 (d, 1H, CH 5', *J=8Hz*), 7.14 (t, 1H, CH 7, *J=8Hz*), 7.33 (m, 1H, CH 6), 7.39 (m, 1H, CH 8), 7.52 (s, 1H, CH 2), 7.60 (d, 1H, CH 9, *J=8Hz*), 8.05 (m, 1H, CH 9), 8.27 (m, 3H, NH_3). ^{13}C-NMR δ (ppm, 100 MHz, DMSO d_6) 40.00 (*CH*$_2$NH$_3$, *CH*$_2$NH), 116.22 (CH 6), 116.69 (CH 5'), 117.73 (CH 2'), 120.06 (Cq 1'), 122.03 (CH 6'), 124.34 (CH 7), 125.75 (Cq 5a), 127.19 (CH 8, CH 9), 132.23 (CH 2), 132.93 to 133.22 (Cq 1, Cq 3a, Cq 9a), 146.18 (Cq 3'), 146.68 (Cq 4'), 147.46 (Cq 4). MS (ESI +, QTof, m/z): 336.15 $[M+H]^+$.

*EAPB02307s: 6-((1-(3,4-dihydroxyphenyl)imidazo[1,2-a]quinoxalin-4-yl)amino)hexan-1-aminium chloride (**10g**).* $C_{22}H_{26}ClN_5O_2$. Mw: 427.93 g/mol. Mp: 214°C. ^{1}H-NMR δ (ppm, 400 MHz, DMSO d_6) 1.39 (m, 4H, *CH*$_2$CH$_2$CH$_2$NH, *CH*$_2$CH$_2$CH$_2$NH$_2$), 1.59 (m, 2H, *CH*$_2$CH$_2$NH$_2$), 1.73 (m, 2H, *CH*$_2$CH$_2$NH), 2.77 (m, 2H, *CH*$_2$NH$_2$), 3.85 (m, 2H, *CH*$_2$NH), 6.81 (d, 1H, CH 6', *J=8Hz*), 6.95 (s, 1H, CH 2'), 6.99 (d, 1H, CH 5', *J=8Hz*), 7.22 (t, 1H, CH 7, *J=8Hz*), 7.34 (d, 1H, CH 6, *J=8Hz*), 7.45 (t, 1H, CH 8 , *J=8Hz*), 7.68 (s, 1H, CH 2), 7.97 (m, 3H, NH_3), 8.35 (m, 1H, CH 9). ^{13}C-NMR δ (ppm, 100 MHz, DMSO d_6) 25.95 and 26.03 (*CH*$_2$CH$_2$CH$_2$NH, *CH*$_2$CH$_2$CH$_2$NH$_2$), 27.23 (*CH*$_2$CH$_2$NH$_2$), 28.44 (*CH*$_2$CH$_2$NH), 40.00 (*CH*$_2$NH$_2$, *CH*$_2$NH), 116.57 (CH 6), 116.71 (CH 5'), 117.61 (CH 2'), 119.60 (CH 9), 120.16 (Cq 1'), 121.82 (CH 6'), 124.19 (CH 7), 125.21 (Cq 5a), 127.52 (CH 8), 131.73 (Cq 1), 134.10 to 134.20 (CH 2, Cq 3a, Cq 9a), 144.88 (Cq 3'), 146.27 (Cq 4'), 147.69 (Cq 4). MS (ESI +, QTof, m/z): 392.21 $[M+H]^+$.

4.2. Cell lines and culture techniques

4.2.1. General

Melanoma (A375) human cancer cell lines were obtained from American Type Culture Collection (Rockville, Md., USA). Cells were cultured in RPMI medium containing RPMI-1640 (Gibco Laboratories, France), 10% heat-inactived (56°C) foetal bovine serum (FBS) (Polylabo, Paris, France), 2 mM L-glutamine, 100 IU/mL penicillin G sodium, 100 mg/mL streptomycin sulfate, and 0.25 mg/mL amphotericin B. Cells were maintained in a humidified atmosphere of 5% CO_2 in air at 37°C.

4.2.2. *In vitro* cytotoxicity assay

Previously to the experiments, the number of cells by well, the doubling time and the MTT concentration have been optimized. In all the experiments, A375 cells were seeded at a final concentration of 5000 cells/well in 96-well microtiter plates and allowed to attach overnight. After 24 h incubation, the medium (phosphate-buffer saline pH 7.3) was aspirated carefully from the plates using a sterile Pasteur pipette, and cells were exposed (i) to vehicle controls (0.15% DMSO/culture medium (v/v) and culture medium alone), (ii) to the synthesized compounds at concentrations of 10^{-5}–$3.2.10^{-9}$ M dissolved in a mixture 0.15% DMSO/culture medium (v/v). After 96 h of incubation, cell supernatant was removed and 100 µL of a MTT (3-[4,5-dimethylthiazol-2-yl]-2,5-diphenyltetrazolium bromide) solution in fresh medium was added per well (MTT final concentration of 0.5 mg/ml) and incubated for 4 h at 37°C. This colorimetric assay is based on the ability of live and metabolically unimpaired tumor-cell targets to reduce MTT to a blue formazan product. At the end of the incubation period, the supernatant was carefully aspirated, then, 100 µL of a mixture of SDS 10% and 0.01 M hydrochloric acid was added to each well. After 2 hours at 37°C of incubation and vigorous shaking to solubilize formazan crystals, the optical density was measured at 570 nm in a microculture plate reader (Dynatech MR 5000, France). For each assay, at least three experiments were performed in triplicate. The individual cell line growth curves confirmed that all A375 lines in control medium remained in the log phase of cell growth 96 h after plating. Cell survival was expressed as percent of vehicle control. The IC_{50} values defined as the concentrations of drugs which produced 50% cell growth inhibition; 50% reduction of absorbance, were estimated from the sigmoidal dose–response curves.

4.3. *In vitro* tubulin polymerization analysis

Tubulin was prepared from pig brain according to the purification procedure described by Williams and Lee.[52,53] To evaluate the effect of the compounds on tubulin assembly *in vitro*, tubulin polymerization was monitored turbidimetrically at 350 nm with a MC2 spectrophotometer (Safas, Monaco) equipped with a thermal-jacketed cuvette holder. The reaction mixture was prepared at 0°C, and contained PEM (Pipes 0.1 M, EGTA 2 mM, $MgSO_4$ 1 mM pH 6.9) buffer, 25% glycerol (v/v), 1 mM GTP, $MgSO_4$ 5 mM, and 12 µM tubulin. GTP and tubulin were added at the very last minute. **EAPB0503**, **EAPB02303** and colchicine stock solutions were diluted in DMSO to the desired concentration, and 2 µL of the compound solution was added to the medium (final concentration: 5 µM). The same volume of DMSO alone was used for negative control. The final volume of the sample was 200 µL. The reaction was started by placing the cuvette in the spectrophotometer cell compartment thermostated at 37°C. Ice was added 45 min later to initiate depolymerization to check for signal specificity.

4.4. Molecular docking assay in the colchicine site

The molecular modeling studies were performed with GOLD.[54] The crystal structure of tubulin complexed with colchicine (PDB 4O2B)[55] was retrieved from the RCSB Protein Data Bank. The binding

sphere with a radius of 25.0 Å was defined with residue Leu255 as the binding site. All compounds were drawn with PRODRG and protonated using BABEL.[56] Finally, they were docked into the binding site using the GOLD protocol with the default settings. The pictures were generated by the program PYMOL.[57]
The docking pose of EAPB0503 was analyzed with two servers (https://projects.biotec.tu-dresden.de/plip-web/plip/index (refX) and https://dockthor.lncc.br/v2/ (refY)) in order to determine a quantitative analysis.

Ref x: PLIP: fully automated protein–ligand interaction profiler

Sebastian Salentin, Sven Schreiber, V. Joachim Haupt, Melissa F. Adasme, Michael Schroeder

Nucleic Acids Res. 2015 Jul 1; 43(Web Server issue): W443–W447. Published online 2015 Apr 14. doi: 10.1093/nar/gkv315

Ref y: K. B. dos Santos, I. A. Guedes, A. L. M. Karl, and L. Dardenne. *Highly Flexible Ligand Docking: Benchmarking of the DockThor Program on the LEADS-PEP Protein-peptide Dataset*, J. Chem. Inf. Model., Jan. 2020, doi: 10.1021/acs.jcim.9b00905.

4.5. *In vitro* transcriptomic study

4.5.1. Experimental design and drug treatments

To explore the mechanism of action of **EAPB02303**, a transcriptomic study was performed. At first, the question of the originality of the mechanism of action was addressed. For this, the A375 cell line was treated without (negative control, drug vehicle: DMSO) or with different Imiqualines derivatives, chemotherapies and targeted therapies used in human clinics at the single concentration of 10 µM for 6 hours in DMEM. Fifteen molecules were used: vemurafenib, dacarbazine, SN38, doxorubicin, fotemustine, 5-FU, methotrexate, vinorelbine, paclitaxel, colchicine, maytansine, Imiquimod, **EAPB02303**, **EAPB0203**, **EAPB0503**. The goal was to compare the mechanisms of action of these different treatments through there associated expression profiles. Then, the expression alterations associated specifically with the **EAPB02303** treatment were further analyzed for mechanistic hypotheses.

4.5.2. RNA isolation and Affymetrix GeneChip processing

Total RNA was extracted from each cell line using RNeasy Mini Kit (Qiagen) according to the manufacturer's protocol. Then, the quality of purified RNA sample was checked with an Agilent BioAnalyzer (Agilent Technologies). Total RNA from each cell line was therefore prepared for hybridization with Affymetrix HG-U133+PM GeneChip according to the manufacturer's protocol in the platform "TRANSCRIPTOME" of Montpellier (IRMB).

4.5.3. Microarray data processing

After hybridization, microarray data were processed with a robust multi-array average (RMA) algorithm as implemented in Expression File Creator module of GenePAttern (Broad Institute). Then, resulting signals were analyzed according to the bioinformatics analysis.

4.5.4. Statistical and Bioinformatics analyses of microarray data

Distances between treatments in the signal space: Morpheus was used to construct a hierarchical clustering of the treatments. First, the signals of each "drug treated" condition were normalized to the control condition (untreated cell signals). Then the resulting values were adjusted according to z-scores method. Finally, the hierarchical clustering was performed using a complete linkage of the expression profiles and Euclidean distances between each pair of treatment were calculated and represented as a dendrogram.

4.6. *In vivo* studies

4.6.1. Animal studies

Animal handling was performed according to guidelines of the Federation of European Laboratory Animal Science Associations (FELASA). This study was performed in compliance with "The French Animal Welfare Act" and following "The French Board for Animal Experiments". This study was performed under approval of the French “Ministère de l’enseignement supérieur et de la recherche” (ethics committee n°CEEA75) in compliance with the "Directive 2010/63/UE.

A375 cells (ATCC; CRL-1619) were cultured in growth medium (DMEM, fetal bovine serum, penicillin-stroptomycin) and diluted every 3-4 days by harvesting in Trypsin. On the injection day, cells were removed from the flasks (by trypsinization), transferred into 50 mL tube, washed with PBS, and then re-suspended in the required amount of PBS to obtain a concentration of 10×10^7 cells/mL. Prior to injection, the cells were pipetted up and down to prevent the presence of cell clumps.

At study initiation, Balb/c-nude mice (Janvier Labs) were inoculated with melanoma cells under anesthesia (isoflurane 1.5-3%). Tumor cells (10×10^6 A375 cells in 100 µL, per animal) were injected into the right flank, subcutaneously, using 1 ml injection syringe with a 25G needle. Tumor measurements (length, width) in mm was performed twice a week starting from Day 4 and thereafter until study termination using a digital caliper. The tumor volume in mm^3 was calculated based on the following formula: Volume = 1/2 x length x $(width)^2$.

Tumors were allowed to grow for two weeks before randomization and group allocation. Treatment started when the average tumor volume reached 110-130 mm^3 by group. All animals were injected intraperitoneally for three weeks. Four groups comprising of 6-12 mice per group were allocated on Day 14 based on tumor measurements. These groups contained a control group treated with vehicle and three treated groups that received **EAPB02303** at the indicated regimen: 75 mg/kg 3 times a week the first week and then twice a week until study termination; 30 mg/kg 5 times a week; 25 mg/kg 3 times a week.

Dosing solutions were prepared on a daily-basis. Stock solution (100 mg/ml) of **EAPB02303** was prepared in DMSO (Sigma), and conserved at (-25) – (-15)°C. The day of injection, the stock solution was diluted in DMSO regarding the final concentration needed. The solution was diluted vol/vol in Tween 80 (Sigma), and divided in aliquots corresponding to the number of mice injected in 15 minutes. Injectable saline (Lavoisier) was added extemporaneously to obtain the final concentrations

needed each 15 minutes. The vehicle was prepared by mixing DMSO and Tween 80 (vol/vol) and injectable saline (8 vol).

4.6.2. Histopathology

Tumors were immersed in buffered 3.7% formalin and evaluated by a veterinary pathologist blinded to the group's treatments during the whole analysis procedure (macroscopic and histologic analyses). The subcutaneous tumors were macroscopically analyzed before and after mid sagittal section. The following criteria were observed: presence or absence of the overlying skin, size (surface) after mid-section, color, consistency and presence of necrosis. After sagittal mid-section, one half of the tumor was embedded in paraffin. Samples were processed with a vacuum infiltration processor and an automated paraffin-embedding system. One 5 µm section was cut using a microtome and a routine trichrome staining (hematoxylin-eosin-saffron) was performed.

Sections were analyzed qualitatively and semi-quantitatively for the following findings: Morphologic type, pigmented or achromic form, fusiform and/or epithelioid morphology; Percentage of necrosis; Mitosis numeration and scoring (performed twice, independently, on 10 high power x 400 fields); Infiltration description and scoring; Stroma scoring; Vascularization scoring; Inflammation scoring; Presence or absence of emboli. The different studied parameters were scored according to the grids presented in the Supplementary Table S3.

4.6.3. Statistics

Analyses were conducted in R[58] using the R packages Rcmdr[59] and PMCR[60] for the post-hoc tests by the Conover and Nemenyi methods.

Statistical analyses were performed using the Kruskal-Wallis rank sum test that generalizes the Mann Whitney Wilcoxon rank sum test to compare multiple independent samples. The Kruskal-Wallis rank sum test is applicable in situations where the distribution assumption in the 1-way Anova is on tenuous and shaky grounds.

The Kruskal-Wallis rank sum (omnibus) test indicates whether at least one of the multiple samples is significantly different (but does not reveal which sample/group is different). Then, a post-hoc test is conducted for pairwise multiple comparison, to discern which of many possible the sample pair combinations are significantly different. For tumor size, tumor weight and mitosis quantification, the post-hoc method of Conover was applied and p-values were adjusted with the superior false discovery rate (FDR) method of Benjaminyi-Hochberg. For animal weight, the post-hoc method of Tukey-Meyer (Nemenyi) was applied without *p*-value adjustment.

For ^{1}H, ^{13}C and ^{19}F NMR spectra, mass spectral data and numerical data for biological tests, please refer to the Supporting Information.

Acknowledgements

Authors thank the Société d'Accélération du Transfert de Technologies (SATT AxLR) for financial support to Cindy Patinote, Stéphanie Paniagua and Johanna Vappiani for technical help, the French

department of Biotage for lending us a HPFC system and 4P Pharma society as subcontractors for the *in vivo* tests.

Authors declare no conflict of interest and no competing financial interest.

Abbreviations used

N,N-DEA, *N,N*-diethylaniline; DIEA, diisopropylethylamine; NaHMDS, sodium bis(trimethylsilylamide); THF, tetrahydrofuran; DMA, dimethylacetamide; ACN, acetonitrile; NBS, N-bromosuccinimide; DME, 1,2-dimethoxyethane; DMSO, dimethylsulfoxyde; IC_{50}, half maximal inhibitory concentration; MM : Multiple Myeloma; MW, microwaves.

References

1. Erdmann F, Lortet-Tieulent J, Schüz J, et al. International trends in the incidence of malignant melanoma 1953-2008--are recent generations at higher or lower risk? *Int J Cancer*. 2013;132(2):385-400. doi:10.1002/ijc.27616
2. Gandini S, Sera F, Cattaruzza MS, et al. Meta-analysis of risk factors for cutaneous melanoma: I. Common and atypical naevi. *Eur J Cancer Oxf Engl 1990*. 2005;41(1):28-44. doi:10.1016/j.ejca.2004.10.015
3. Gandini S, Sera F, Cattaruzza MS, et al. Meta-analysis of risk factors for cutaneous melanoma: II. Sun exposure. *Eur J Cancer Oxf Engl 1990*. 2005;41(1):45-60. doi:10.1016/j.ejca.2004.10.016
4. Gandini S, Sera F, Cattaruzza MS, et al. Meta-analysis of risk factors for cutaneous melanoma: III. Family history, actinic damage and phenotypic factors. *Eur J Cancer Oxf Engl 1990*. 2005;41(14):2040-2059. doi:10.1016/j.ejca.2005.03.034
5. Barbaric J, Sekerija M, Agius D, et al. Disparities in melanoma incidence and mortality in South-Eastern Europe: Increasing incidence and divergent mortality patterns. Is progress around the corner? *Eur J Cancer*. 2016;55:47-55. doi:10.1016/j.ejca.2015.11.019
6. Allemani C, Matsuda T, Di Carlo V, et al. Global surveillance of trends in cancer survival 2000–14 (CONCORD-3): analysis of individual records for 37 513 025 patients diagnosed with one of 18 cancers from 322 population-based registries in 71 countries. *The Lancet*. 2018;391(10125):1023-1075. doi:10.1016/S0140-6736(17)33326-3
7. Sacchetto L, Zanetti R, Comber H, et al. Trends in incidence of thick, thin and in situ melanoma in Europe. *Eur J Cancer*. 2018;92:108-118. doi:10.1016/j.ejca.2017.12.024
8. Algazi AP, Soon CW, Daud AI. Treatment of cutaneous melanoma: current approaches and future prospects. *Cancer Manag Res*. 2010;2:197-211. doi:10.2147/CMR.S6073
9. Kwong A, Sanlorenzo M, Rappersberger K, Vujic I. Update on advanced melanoma treatments: small molecule targeted therapy, immunotherapy, and future combination therapies. *Wien Med Wochenschr 1946*. January 2017. doi:10.1007/s10354-016-0535-1
10. Drugs Approved for Melanoma. National Cancer Institute. https://www.cancer.gov/about-cancer/treatment/drugs/melanoma. Accessed December 11, 2017.
11. Glitza IC, Kim DW, Chae YK, Kim KB. Targeted Therapy in Melanoma. In: *Genetics of Melanoma*. Cancer Genetics. Springer, New York, NY; 2016:237-265. doi:10.1007/978-1-4939-3554-3_11
12. Hauschild A, Agarwala SS, Trefzer U, et al. Results of a phase III, randomized, placebo-controlled study of sorafenib in combination with carboplatin and paclitaxel as second-line treatment in patients with unresectable stage III or stage IV melanoma. *J Clin Oncol Off J Am Soc Clin Oncol*. 2009;27(17):2823-2830. doi:10.1200/JCO.2007.15.7636

13. Chapman PB, Hauschild A, Robert C, et al. Improved survival with vemurafenib in melanoma with BRAF V600E mutation. *N Engl J Med*. 2011;364(26):2507-2516. doi:10.1056/NEJMoa1103782
14. Hauschild A, Grob J-J, Demidov LV, et al. Dabrafenib in BRAF-mutated metastatic melanoma: a multicentre, open-label, phase 3 randomised controlled trial. *Lancet Lond Engl*. 2012;380(9839):358-365. doi:10.1016/S0140-6736(12)60868-X
15. Robert C, Karaszewska B, Schachter J, et al. Improved Overall Survival in Melanoma with Combined Dabrafenib and Trametinib. *N Engl J Med*. 2015;372(1):30-39. doi:10.1056/NEJMoa1412690
16. Ribas A, Gonzalez R, Pavlick A, et al. Combination of vemurafenib and cobimetinib in patients with advanced BRAF(V600)-mutated melanoma: a phase 1b study. *Lancet Oncol*. 2014;15(9):954-965. doi:10.1016/S1470-2045(14)70301-8
17. Long GV, Stroyakovskiy D, Gogas H, et al. Combined BRAF and MEK inhibition versus BRAF inhibition alone in melanoma. *N Engl J Med*. 2014;371(20):1877-1888. doi:10.1056/NEJMoa1406037
18. Hodi FS, Corless CL, Giobbie-Hurder A, et al. Imatinib for Melanomas Harboring Mutationally Activated or Amplified KIT Arising on Mucosal, Acral, and Chronically Sun-Damaged Skin. *J Clin Oncol*. 2013;31(26):3182-3190. doi:10.1200/JCO.2012.47.7836
19. Pardoll DM. The blockade of immune checkpoints in cancer immunotherapy. *Nat Rev Cancer*. 2012;12(4):252-264. doi:10.1038/nrc3239
20. Azijli K, Stelloo E, Peters GJ, VAN DEN Eertwegh AJM. New developments in the treatment of metastatic melanoma: immune checkpoint inhibitors and targeted therapies. *Anticancer Res*. 2014;34(4):1493-1505.
21. Ott PA, Hodi FS, Robert C. CTLA-4 and PD-1/PD-L1 blockade: new immunotherapeutic modalities with durable clinical benefit in melanoma patients. *Clin Cancer Res Off J Am Assoc Cancer Res*. 2013;19(19):5300-5309. doi:10.1158/1078-0432.CCR-13-0143
22. Kirkwood JM, Tarhini AA, Panelli MC, et al. Next generation of immunotherapy for melanoma. *J Clin Oncol Off J Am Soc Clin Oncol*. 2008;26(20):3445-3455. doi:10.1200/JCO.2007.14.6423
23. Belardelli F, Ferrantini M, Proietti E, Kirkwood JM. Interferon-alpha in tumor immunity and immunotherapy. *Cytokine Growth Factor Rev*. 2002;13(2):119-134. doi:10.1016/S1359-6101(01)00022-3
24. Bong AB, Bonnekoh B, Franke I, Schön MP, Ulrich J, Gollnick H. Imiquimod, a topical immune response modifier, in the treatment of cutaneous metastases of malignant melanoma. *Dermatol Basel Switz*. 2002;205(2):135-138. doi:10.1159/000063904
25. Ellis LZ, Cohen JL, High W, Stewart L. Melanoma in situ treated successfully using imiquimod after nonclearance with surgery: review of the literature. *Dermatol Surg Off Publ Am Soc Dermatol Surg Al*. 2012;38(6):937-946. doi:10.1111/j.1524-4725.2012.02362.x
26. Harrison CJ, Jenski L, Voychehovski T, Bernstein DI. Modification of immunological responses and clinical disease during topical R-837 treatment of genital HSV-2 infection. *Antiviral Res*. 1988;10(4):209-223. doi:10.1016/0166-3542(88)90032-0
27. Deleuze-Masquefa C, Moarbess G, Khier S, et al. New imidazo[1,2-a]quinoxaline derivatives: synthesis and in vitro activity against human melanoma. *Eur J Med Chem*. 2009;44(9):3406-3411. doi:10.1016/j.ejmech.2009.02.007
28. Moarbess G, Deleuze-Masquefa C, Bonnard V, et al. In vitro and in vivo anti-tumoral activities of imidazo[1,2-a]quinoxaline, imidazo[1,5-a]quinoxaline, and pyrazolo[1,5-a]quinoxaline derivatives. *Bioorg Med Chem*. 2008;16(13):6601-6610. doi:10.1016/j.bmc.2008.05.022

29. Deleuze-Masquéfa C, Gerebtzoff G, Subra G, et al. Design and synthesis of novel imidazo[1,2-a]quinoxalines as PDE4 inhibitors. *Bioorg Med Chem*. 2004;12(5):1129-1139. doi:10.1016/j.bmc.2003.11.034
30. Deleuze-Masquefa C, Moarbess G, Bonnet P-A, Pinguet F, Bazarbachi A, Bressolle F. Imidazo[1,2-a]quinoxalines and derivatives for the treatment of cancers. Patent WO2009043934 A1. 2009.
31. Zghaib Z, Guichou J-F, Vappiani J, et al. New imidazoquinoxaline derivatives: Synthesis, biological evaluation on melanoma, effect on tubulin polymerization and structure–activity relationships. *Bioorg Med Chem*. 2016;24(11):2433-2440. doi:10.1016/j.bmc.2016.04.004
32. Courbet A, Bec N, Constant C, et al. Imidazoquinoxaline anticancer derivatives and imiquimod interact with tubulin: Characterization of molecular microtubule inhibiting mechanisms in correlation with cytotoxicity. *PLOS ONE*. 2017;12(8):e0182022. doi:10.1371/journal.pone.0182022
33. Lu Y, Chen J, Xiao M, Li W, Miller DD. An overview of tubulin inhibitors that interact with the colchicine binding site. *Pharm Res*. 2012;29(11):2943-2971. doi:10.1007/s11095-012-0828-z
34. Patinote C, Bou Karroum N, Moarbess G, et al. Imidazo[1,2-a]pyrazine, Imidazo[1,5-a]quinoxaline and Pyrazolo[1,5-a]quinoxaline derivatives as IKK1 and IKK2 inhibitors. *Eur J Med Chem*. 2017;138:909-919. doi:10.1016/j.ejmech.2017.07.021
35. Moarbess G, Guichou J-F, Paniagua-Gayraud S, et al. New IKK inhibitors: Synthesis of new imidazo[1,2-a]quinoxaline derivatives using microwave assistance and biological evaluation as IKK inhibitors. *Eur J Med Chem*. 2016;115:268-274. doi:10.1016/j.ejmech.2016.03.006
36. Cuq P, Deleuze-Masquefa C, Bonnet P-A, Patinote C. New imidazo[1,2-a]quinoxalines and derivatives for the treatment of cancers. Patent WO2016107895 A1. 2016.
37. Lenzi O, Colotta V, Catarzi D, et al. Synthesis, structure–affinity relationships, and molecular modeling studies of novel pyrazolo[3,4-c]quinoline derivatives as adenosine receptor antagonists. *Bioorg Med Chem*. 2011;19(12):3757-3768. doi:10.1016/j.bmc.2011.05.001
38. Parra S, Laurent F, Subra G, et al. Imidazo[1,2-a]quinoxalines: synthesis and cyclic nucleotide phosphodiesterase inhibitory activity. *Eur J Med Chem*. 2001;36(3):255-264. doi:10.1016/S0223-5234(01)01213-2
39. Cherng Y-J. Efficient nucleophilic substitution reactions of quinolyl and isoquinolyl halides with nucleophiles under focused microwave irradiation. *Tetrahedron*. 2002;58(6):1125-1129. doi:10.1016/S0040-4020(01)01225-X
40. Wuts PGM, Greene TW. *Greene's Protective Groups in Organic Synthesis*. John Wiley & Sons; 2006.
41. Greene TW, Wuts PGM. Protection for the Hydroxyl Group, Including 1,2- and 1,3-Diols. In: *Protective Groups in Organic Synthesis*. John Wiley & Sons, Inc.; 1999:23. doi:10.1002/0471220574.ch2
42. Perspicace E, Giorgio A, Carotti A, Marchais-Oberwinkler S, Hartmann RW. Novel N-methylsulfonamide and retro-N-methylsulfonamide derivatives as 17β-hydroxysteroid dehydrogenase type 2 (17β-HSD2) inhibitors with good ADME-related physicochemical parameters. *Eur J Med Chem*. 2013;69:201-215. doi:10.1016/j.ejmech.2013.08.026
43. Perspicace E, Cozzoli L, Gargano EM, et al. Novel, potent and selective 17β-hydroxysteroid dehydrogenase type 2 inhibitors as potential therapeutics for osteoporosis with dual human and mouse activities. *Eur J Med Chem*. 2014;83:317-337. doi:10.1016/j.ejmech.2014.06.036
44. Koppitz M, Klar U, Jautelat R, et al. Substituted 6-imidazopyrazines for use as mps-1 and tkk inhibitors in the treatment of hyperproliferative disorders. June 2012. http://google.com/patents/WO2012080234A1. Accessed January 19, 2018.
45. Klar U, Koppitz M, Kosemund D, et al. Imidazopyrazines. WO 2011/113862 A1. The Lens. https://www.lens.org/lens. Accessed January 19, 2018.

46. Goel R, Luxami V, Paul K. Recent advances in development of imidazo[1,2-a]pyrazines: synthesis, reactivity and their biological applications. *Org Biomol Chem*. 2015;13(12):3525-3555. doi:10.1039/C4OB01380H
47. Macleod A, Mitchell DR, Palmer NJ, et al. *Imidazo [1,2-a] Pyrazine Compounds for Treatment of Viral Infections Such as Hepatitis*.; 2008. https://www.google.com/patents/WO2009024585A2?cl=und. Accessed January 19, 2018.
48. Parmenter TJ, Kleinschmidt M, Kinross KM, et al. Response of BRAF-Mutant Melanoma to BRAF Inhibition Is Mediated by a Network of Transcriptional Regulators of Glycolysis. *Cancer Discov*. 2014;4(4):423-433. doi:10.1158/2159-8290.CD-13-0440
49. Research AA for C. BRAF Silencing by Short Hairpin RNA or Chemical Blockade by PLX4032 Leads to Different Responses in Melanoma and Thyroid Carcinoma Cells. *Mol Cancer Res*. May 2008. doi:10.1158/1541-7786.MCR-07-2001
50. Li Y-Y. BRAF Inhibitor (Vemurafenib) Resistance Confers Sensitivity to Arginine Deprivation in Melanoma. *Open Access Diss*. March 2016. https://scholarlyrepository.miami.edu/oa_dissertations/1603.
51. Drug Download Page - Cancerrxgene - Genomics of Drug Sensitivity in Cancer. https://www.cancerrxgene.org/downloads/bulk_download. Accessed January 17, 2020.
52. Hamel E, Lin CM. Separation of active tubulin and microtubule-associated proteins by ultracentrifugation and isolation of a component causing the formation of microtubule bundles. *Biochemistry*. 1984;23(18):4173-4184. doi:10.1021/bi00313a026
53. Williams RC, Lee JC. Preparation of tubulin from brain. *Methods Enzymol*. 1982;85 Pt B:376-385. doi:10.1016/0076-6879(82)85038-6
54. Korb O, Stützle T, Exner TE. PLANTS: Application of Ant Colony Optimization to Structure-Based Drug Design. In: Dorigo M, Gambardella LM, Birattari M, Martinoli A, Poli R, Stützle T, eds. *Ant Colony Optimization and Swarm Intelligence*. Lecture Notes in Computer Science. Springer Berlin Heidelberg; 2006:247-258.
55. Prota AE, Danel F, Bachmann F, et al. The novel microtubule-destabilizing drug BAL27862 binds to the colchicine site of tubulin with distinct effects on microtubule organization. *J Mol Biol*. 2014;426(8):1848-1860. doi:10.1016/j.jmb.2014.02.005
56. Schüttelkopf AW, van Aalten DMF. PRODRG: a tool for high-throughput crystallography of protein–ligand complexes. *Acta Crystallogr D Biol Crystallogr*. 2004;60(8):1355-1363. doi:10.1107/S0907444904011679
57. PyMOL | pymol.org. https://pymol.org/2/. Accessed September 19, 2019.
58. R Core Team. *R: A Language and Environment for Statistical Computing. R Foundation for Statistical Computing*. Vienna, Austria. https://www.R-project.org.
59. Fox J, Bouchet-Valat M. *Rcmdr: R Commander. R Package.*; 2019.
60. Pohlet T. *The Pairwise Multiple Comparison of Mean Ranks Package (PMCMR). R Package.*; 2014. https://CRAN.R-project.org/package=PMCMR.